# Can we detect changes in the fluid network near the slab interface during the ETS cycle by continuous magnetotelluric monitoring?

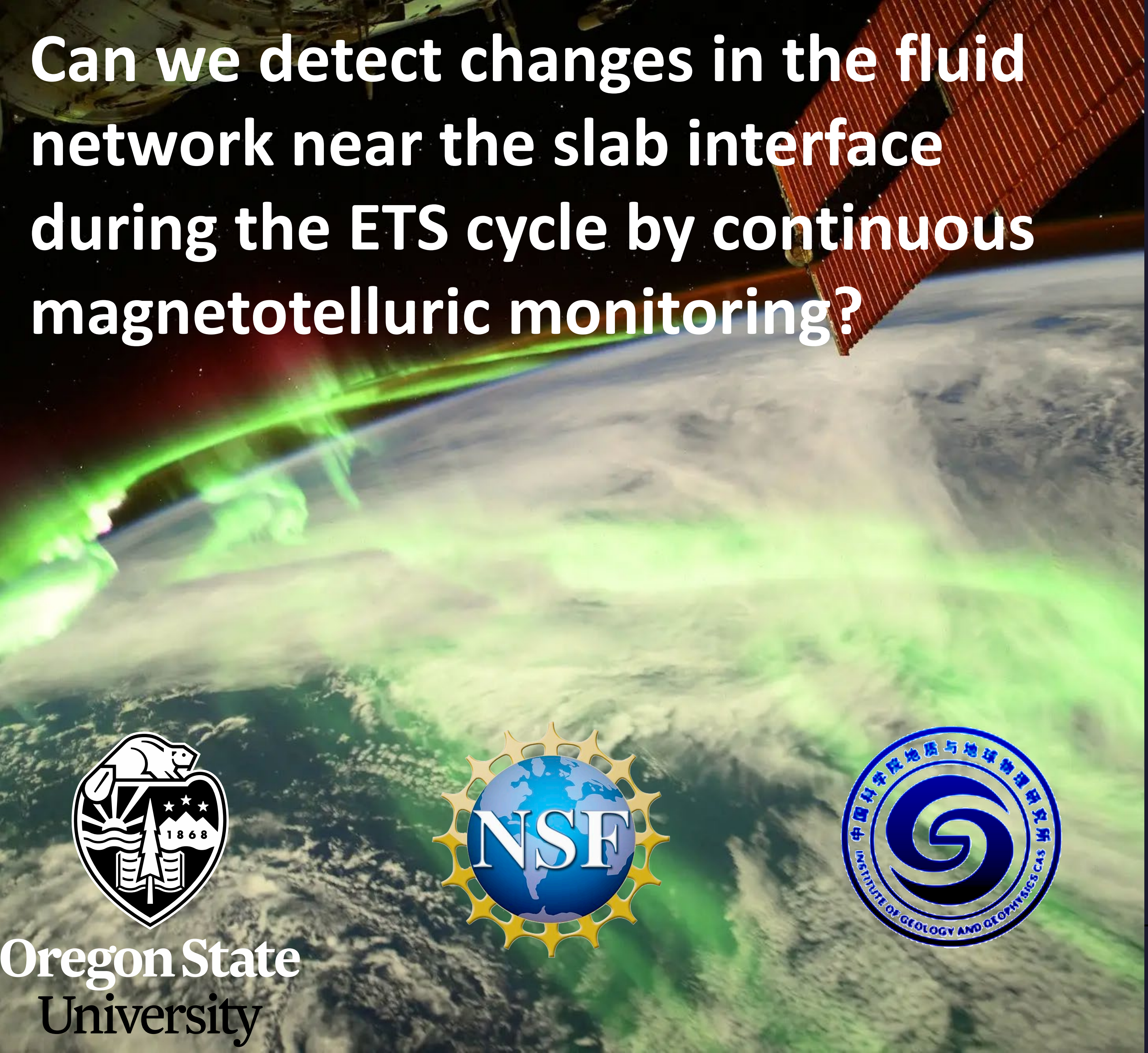

CRESCENT
CASCADIA REGION EARTHQUAKE SCIENCE CENTER

**Adam Schultz[1]**

**(Overview & Context)**

**Xiaolei Tu[1,2]**

**(Numerical Simulations)**

[1]College of Earth, Ocean and Atmospheric Sciences

Oregon State University

[1,2]Institute of Geology and Geophysics

Chinese Academy of Sciences

04/24/2025

# Episodic Tremor and Slip (ETS)

The infrequency of large earthquakes along the Cascadia margin complicates efforts to validate physical models of plate dynamics. ETS - episodic, repeating( ~14 mo between Seattle and Vancouver) low magnitude tremor with stress release by slip rather than rupture provides a recurring window into the relationship between changes in the fluid/rock system near  the slab/mantle wedge interface to changes in the stress field and to the strain and displacement within that boundary zone that results.

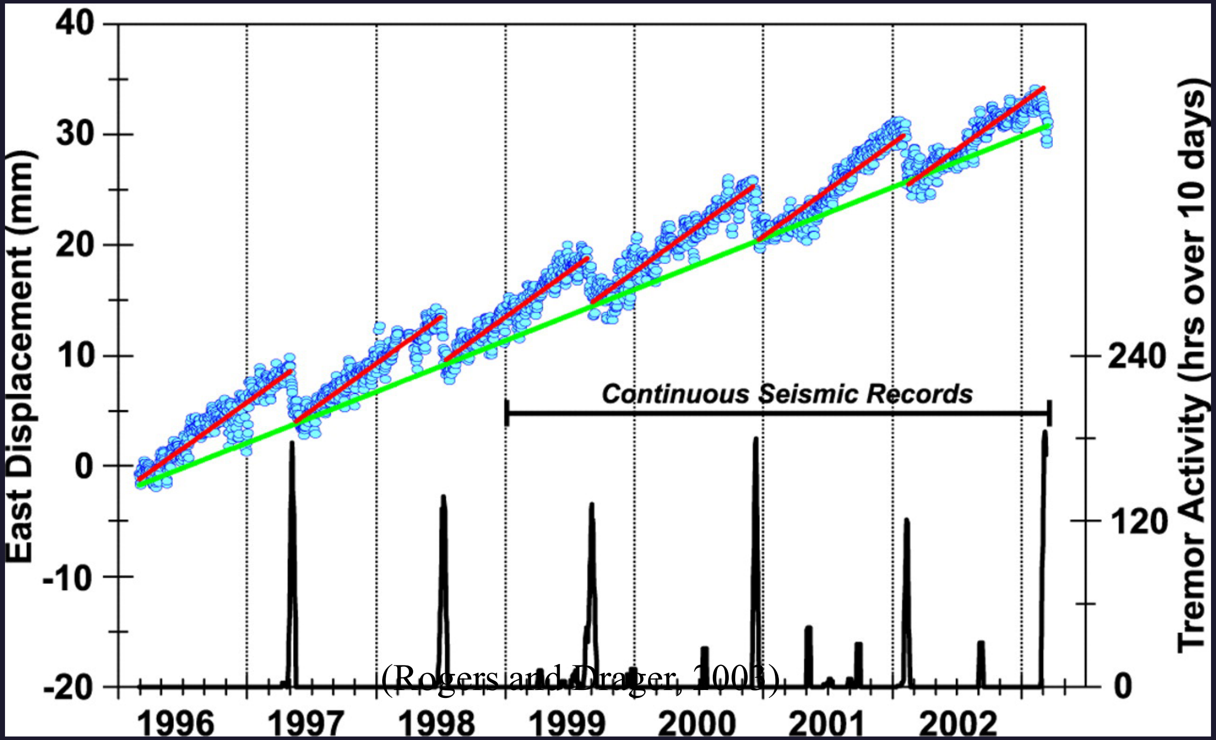


**ETS zone at Cascadia subduction zone**

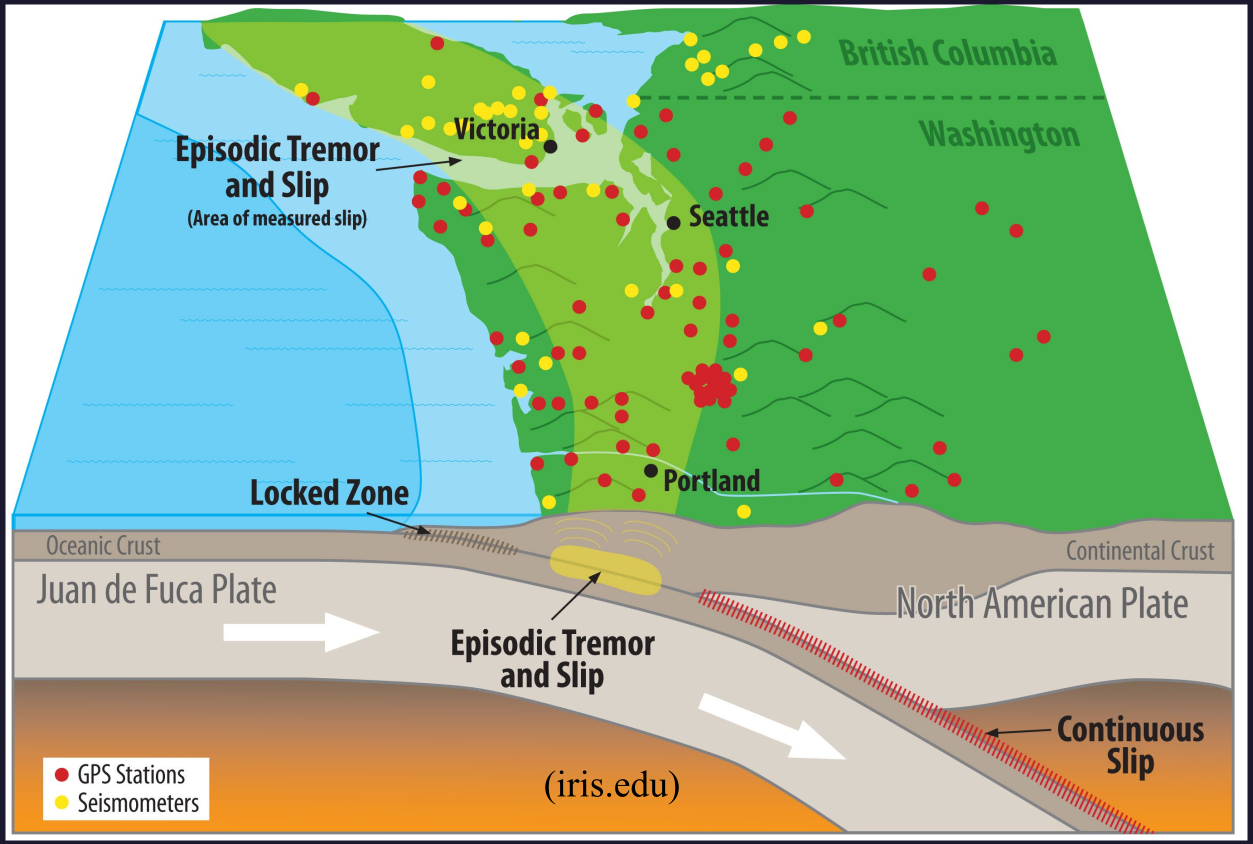

# A Fluid-driven Mechanism?

Seismic observations indicate ETS events may be controlled by the **presence** of, and possible **fluctuations** in pore-fluid pressure.

The fluid-driven model posits **cyclic fluid release and migration** in sync with ETS episodes. We consider that possibility**, <u>but also another</u>** that the lubrication of the plate interface might be related to realignment of fluid filled channels in response to changes in the stress field due to plate **<u>kinematics</u>**, thereby changing the shear strength along the slab interface.

Seismic and geodetic data **lack direct sensitivity** to these fluids, at these depths and scale lengths. There is **a significant gap** in direct observations of fluid movements or the realignment of fluid-filled channels associated with ETS.

## ETS cycle and fluid movements

**Intra-ETS:** brittle failure & fluid release
**Inter-ETS:** fluid recharge & pore pressure buildup

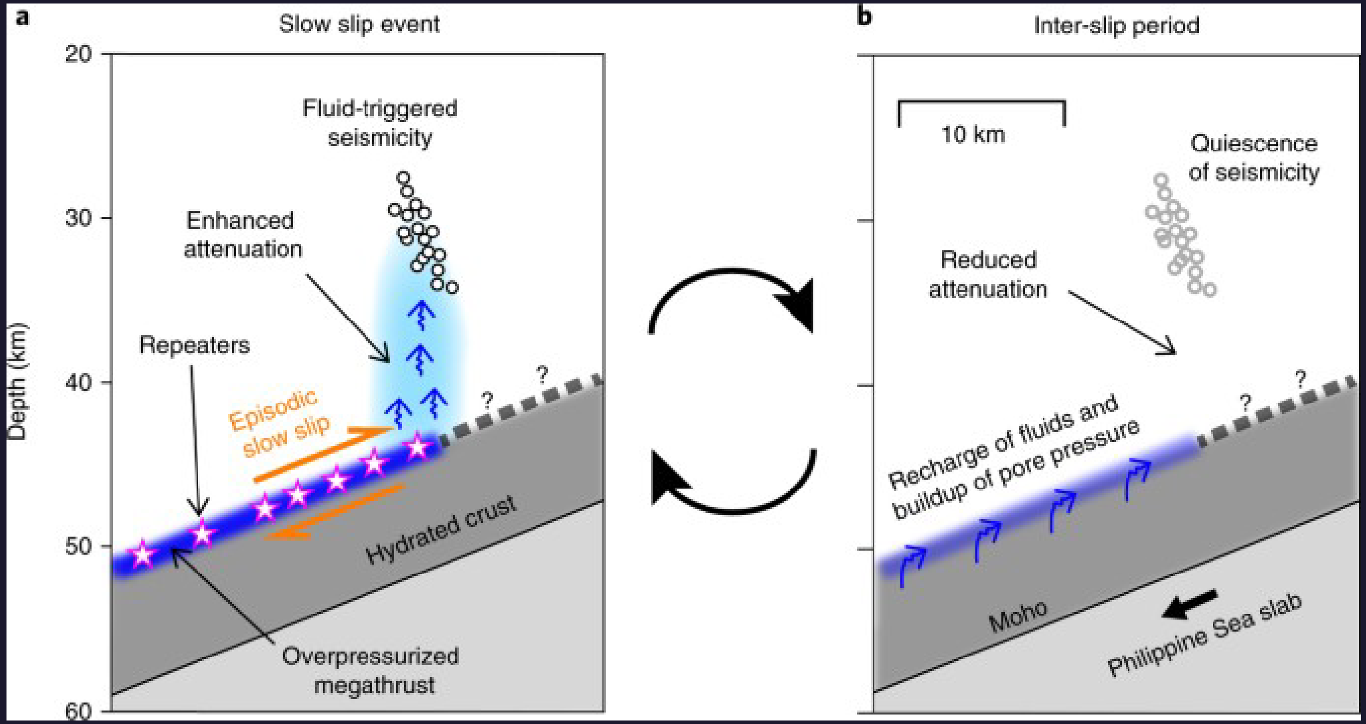


(Nakajima and Uchida, 2018)

# Electrical resistivity in Earth materials:

- (Mg,Fe)-Al silicates are impure semi-conductors, doped by the presence of various contaminates
- Electrical conduction is both a material bulk property, and a crystal grain boundary property
- Bulk conduction depends on rock composition and temperature, and to a lesser extent on pressure
- Grain boundary conduction is strongly influenced by fluids (interconnected partial melt and aqueous solutions), volatiles, carbon

The electrical conductivity (1/resistivity) is a function of the conductivity of the fluids/films/dopants along the grain boundaries and the bulk conductivity of the mineral grains

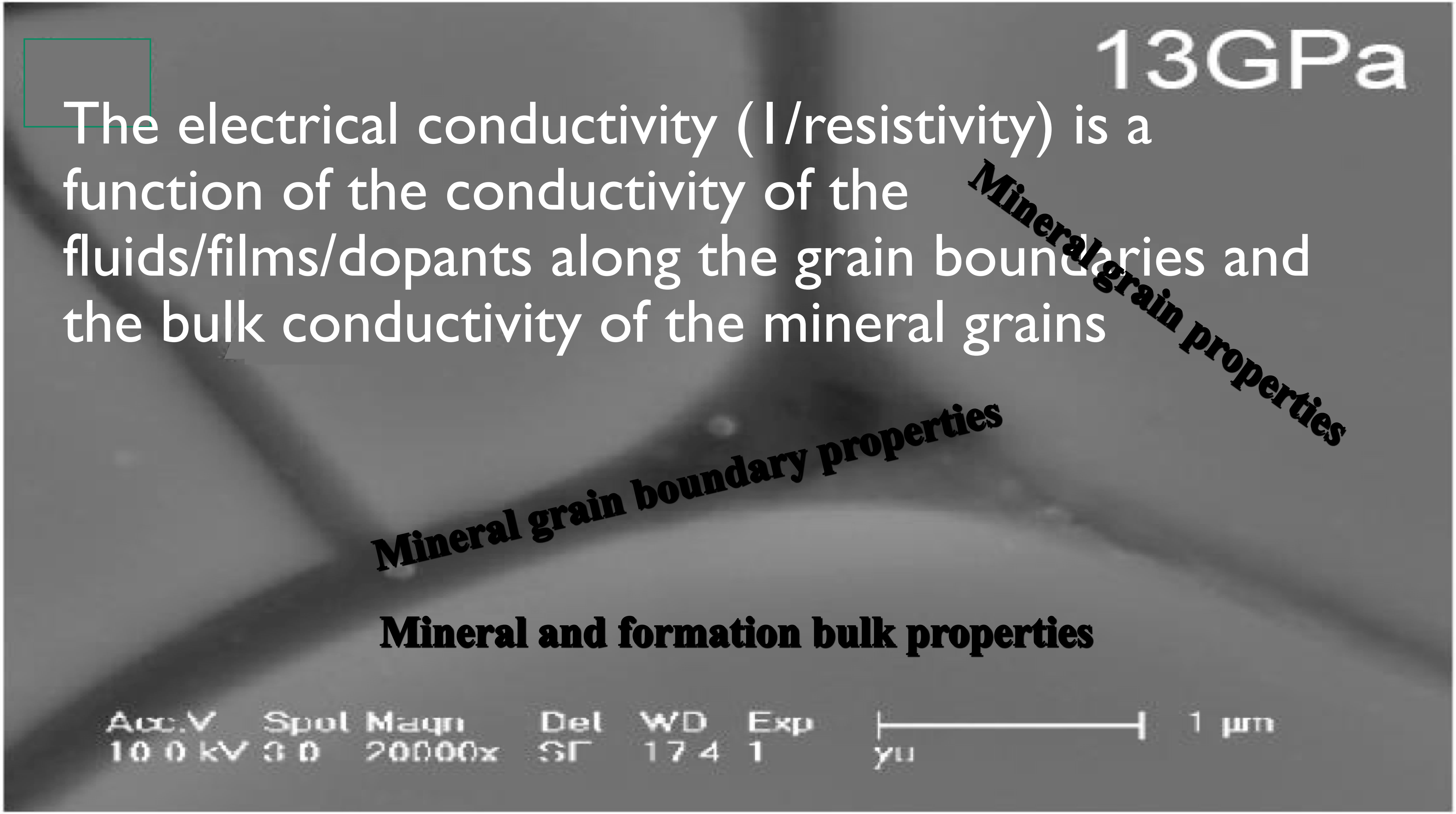

# Electrical resistivity in Earth materials:

*In situ* crustal conductivities may be enhanced by saline fluids and/or graphite, metallic oxides and sulphides, or partial melt. Mantle conductivities may be enhanced by fluids (including partial melts), graphite or hydrogen diffusivity (see Sections 9.2 and 9.3). Macroscopic anisotropy is most easily explained if conductive phases are preferentially aligned (e.g., owing to crystal-preferred orientation) or exhibit a higher degree of interconnection in the more conductive direction.

Graphitic films have been observed in metamorphic rocks using Auger electron emission spectroscopy (Frost *et al.*, 1989). Amphibolite and gneiss core samples from depths of between

**Figure 8.2** Macroscopic fabric elements of mylonite rock samples from the Indian Ocean ridge and their direction-dependent electrical resistivities. The values in brackets are for low pressures, corresponding to shallow crustal depths, whilst the other values are for the high pressures expected at deeper crustal depths. The resistivities of these rock samples are too high, and their anisotropies too low to explain deep-crustal conductivity anomalies revealed by MT field measurements. (Redrawn from Siegesmund *et al.*, 1991.)

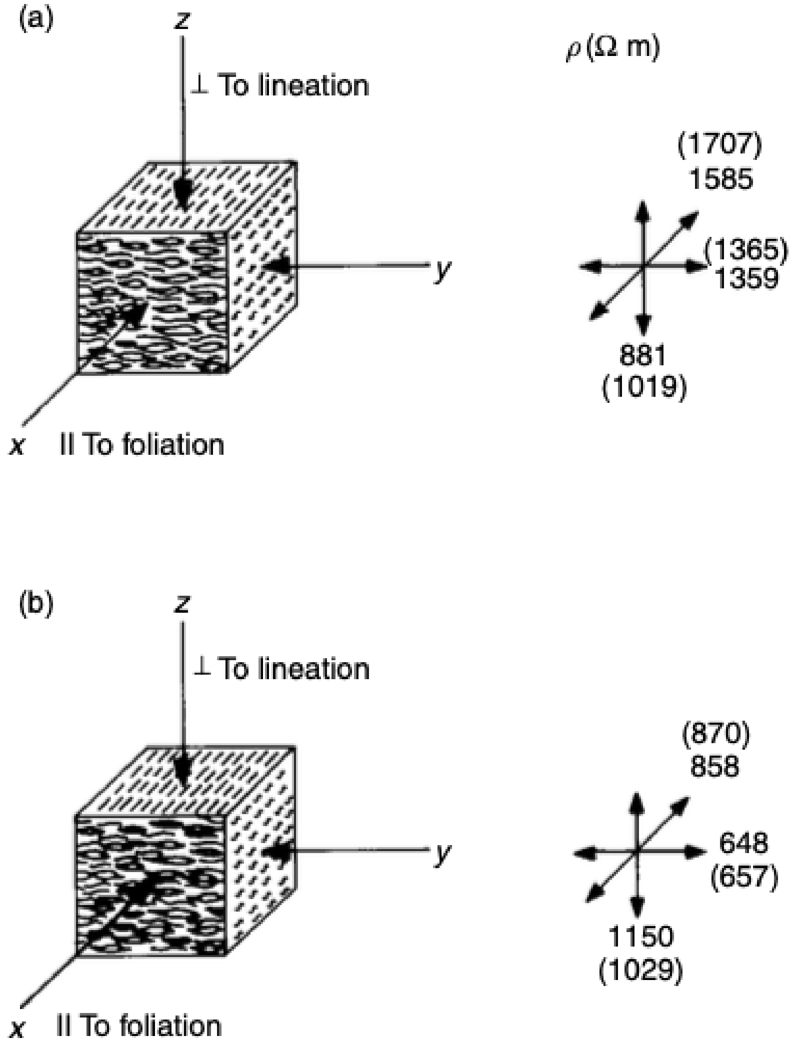


Excerpts from Simpson and Bahr, *Practical Magnetotellurics,* Cambridge University Press, 2010. (right) note anisotropic effects on conductivity.

# Electrical resistivity in Earth materials:

Empirical scaling relationships represent the conductivity (1/resistivity) of a porous material composed of solid grains with pores (partially filled) with fluids of a given conductivity. At shallow depths, such as in marine and near-surface saturated sediments, electronic conduction across the solid grains is negligible compared to electrolytic conduction through the pores.

Archie's Law (Archie, 1942) is most commonly used to represent the electrolytic conduction:

$$\sigma = \phi^m \sigma_e,$$

Where $\sigma_e$ is the conductivity ($1/\rho_e$) of the electrolytic fluid, $\Phi$ **is the porosity** of the medium, and the constant *m ("cementation factor")* depends on the shape and connectivity of the pores. *m≈1* for interconnected, low aspect ratio cracks, *m≈2* for poorly connected, high aspect ratio cracks. In the higher lithostatic pressure of the mid-crust, intermediate geometries hold where *m≈1.5.*

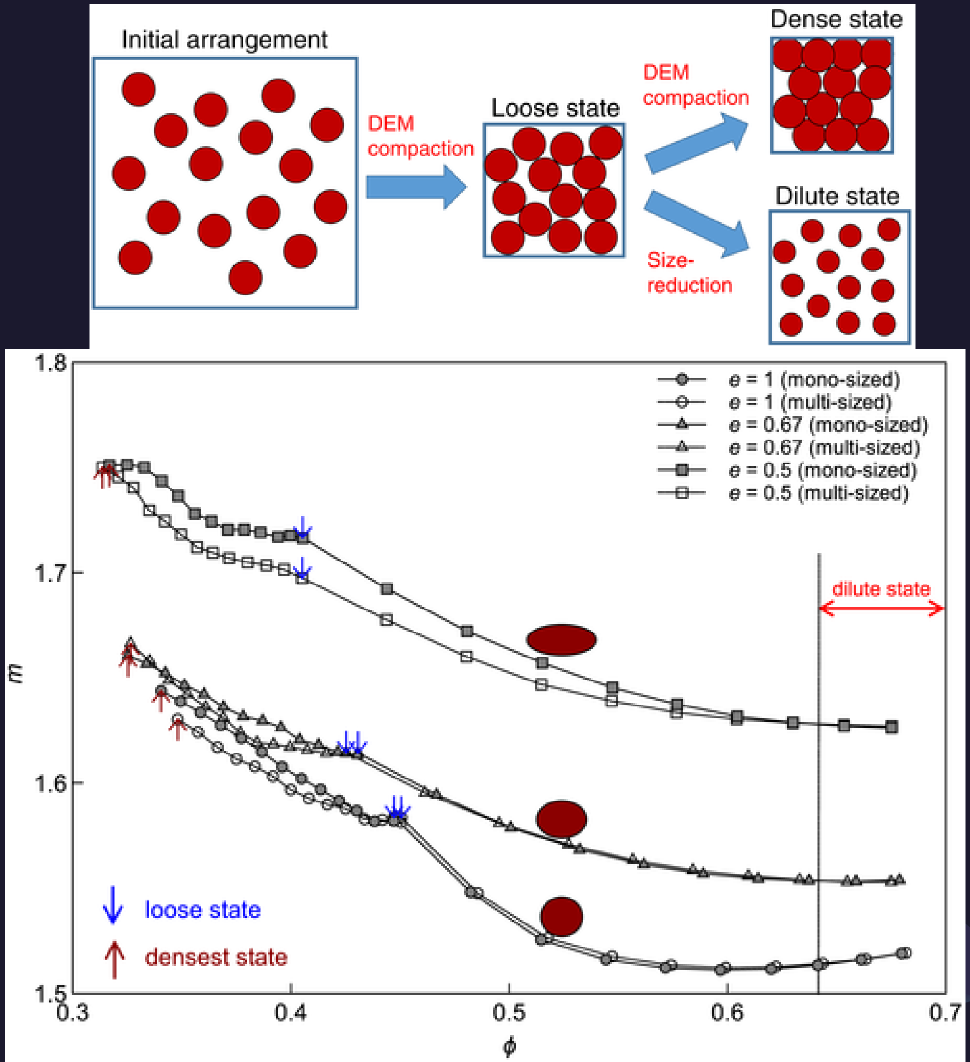


Source: Q. Niu & C. Zhang, 2018, https://doi.org/10.1002/2017GL076751

# Electrical resistivity in Earth materials:

As porosity $\Phi$ decreases to a critical level the conductivity of the solid rock matrix $\sigma_r$ can no longer be disregarded and Archie's Law is modified:

$$\sigma = \sigma_r + \phi^2 \left(\sigma_e - \sigma_r\right).$$

At even greater depths in the lower crust and the mantle, minerals become semi-conductors and the conductivity of the mineral grains, $\sigma_r$ becomes temperature dependent following the Arrhenius equation:

$$\sigma_r = \sigma_0 e^{-E_A/k_B T},$$

where $E_A$ is the activation energy, $k_B$ is Boltzmann's constant, and $\sigma_0$ is the conductivity as $T \rightarrow \infty$. Under these high-pressure conditions $\sigma_e$ represents the conductivity of melt or volatiles that may exist along the grain boundaries.

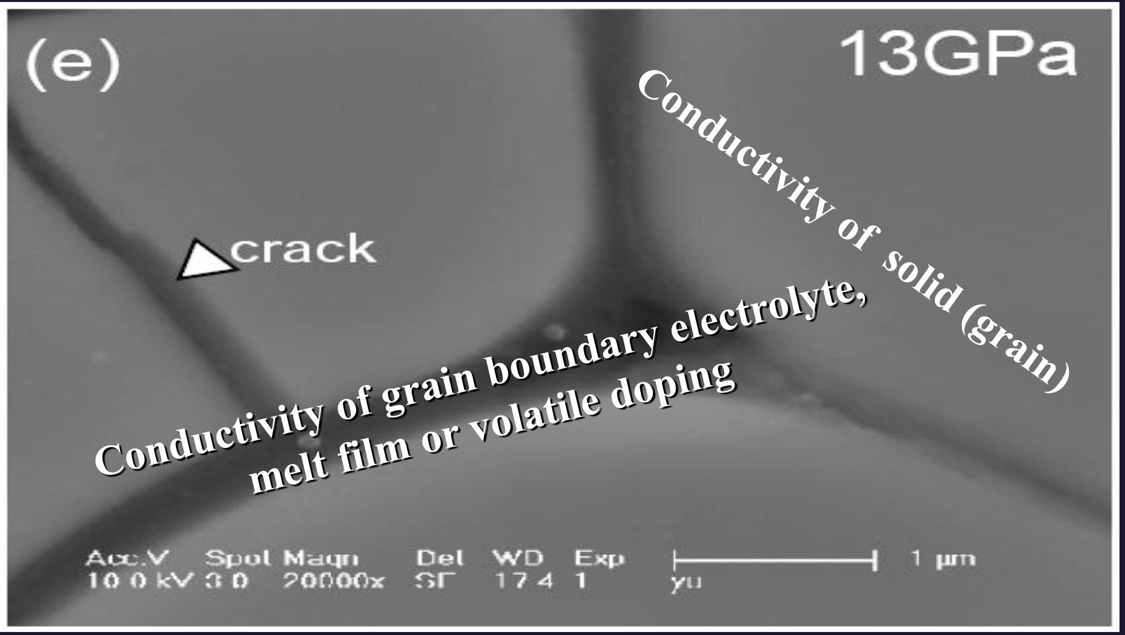


The bulk conductivity of a two-phase medium can be reasonably approximated through Archie's Law, or through alternatives such as the Hashin-Sktrikmann, 1962) upper and lower bounds on bulk conductivity model.

# Temporal changes in electrical conduction at the slab interface and lower mantle wedge

Several mechanisms relevant to this workshop may impact electrical conduction within the down-going slab/mantle wedge **to a significant degree** during the EQ & ETS cycle. Key amongst these are:

1 )Bulk changes in fluid volume and distribution – fluid overpressuring as a “lubricant” along the interface (or fluid chemistry over long term) and/or

2) Distortions in the fabric of interconnected channels along grain boundaries – $\Delta\sigma,\tau$ {stress changes} $\rightarrow \Delta\varepsilon,\gamma$ {strain changes, i.e. compression, shearing, rotation, channel orientation}

**An example for Oaxaca (Villafuerte, et al. (2025):** Coulomb Failure Stress (CFS) contributions by regions in coupling regime and relaxing slip. (a) and (b) show the cumulative CFS ...

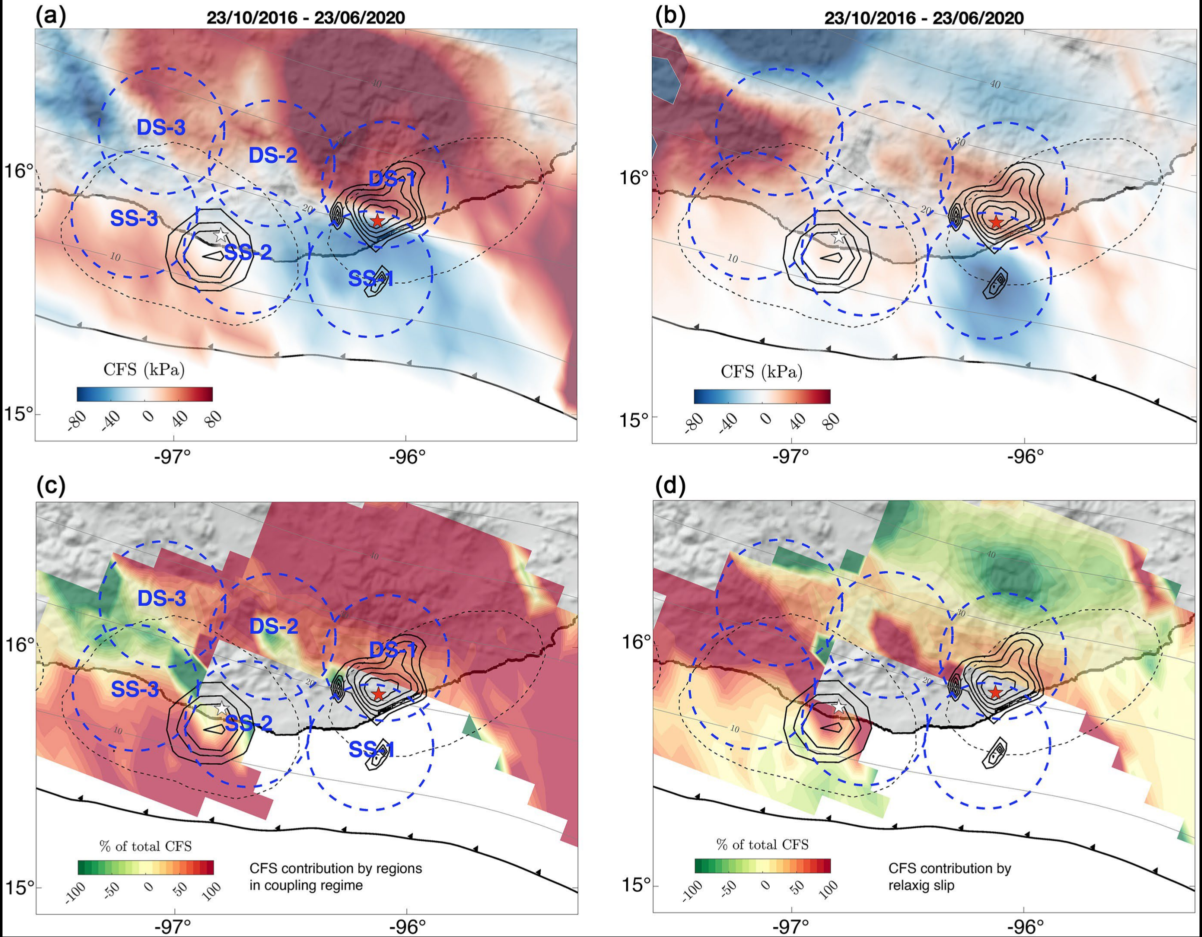


"pre-seismic, coseismic and post-seismic phases associated with the 2020 June 23 Mw 7.4 Huatulco earthquake... continuous changes in both the aseismic stress-releasing slip and the coupling produced a high stress concentration [i.e. Coulomb failure stress (CFS) of **80 kPa (~12 psi)**[1] prior to the event on the region with the highest moment release of the Huatulco earthquake (between 17 and 30 km depth) and a stress deficit zone in the adjacent updip region (i.e. shallower than 17 km depth with CFS around −90 kPa (~-13 psi). This region under negative stress accumulation can be explained by possible recurrent shallow slow slip events (SSE) offshore Huatulco as well as by the stress shadow from adjacent locked segments... Throughout the 4-yr period analysed, the interface region of the 1978 event experienced a **high CFS build up of 80–150 kPa**, primarily attributable to both the coseismic and early post-seismic slip of the Huatulco rupture

[1] I find such CFS levels remarkably small considering pressures required to hydroshear or hydrofrac rock in EGS systems exceeds 20 Mpa.

*Geophys J Int*, Volume 241, Issue 1, April 2025, Pages 17–34, https://doi.org/10.1093/gji/ggaf022

# Can we monitor changes in the fluid/rock matrix during EQ and ETS cycles?

Let's talk about… Magnetotellurics!

# The Magnetotelluric Method – 3-D/4-D imaging

By measuring the vector electric and magnetic fields at the Earth's surface, we determine the frequency dependent *impedance tensor*, which we use to image the electrical resistivity structure of the **near-surface** through the **upper mantle.**

(left) installing a long-period MT data acquisition system; (right) the two horizontal electric field dipole sensors and two horizontal and one vertical magnetic field sensor.

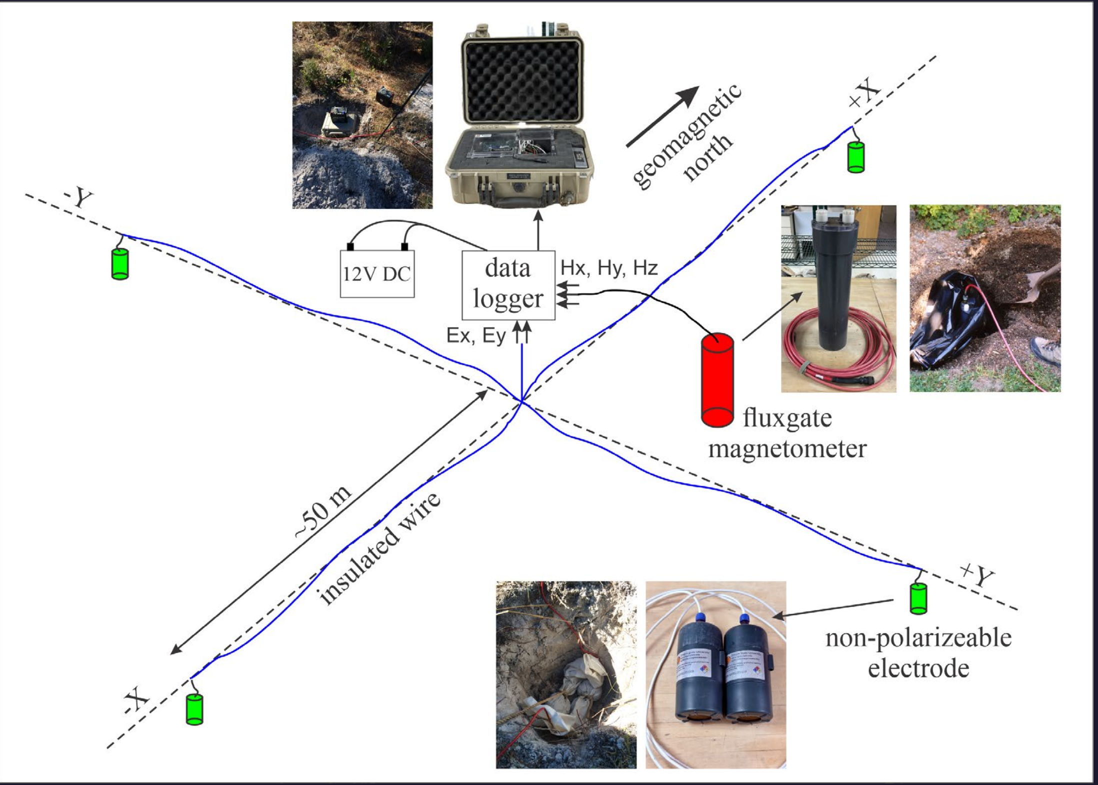


Figure from Kelbert, et al., *Rev. Geophys.*, in prep, 2025.

# The Magnetotelluric Method (MT)

We measure two orthogonal horizontal electric field components $E_x(t)$ and $E_y(t)$, and three orthogonal magnetic field components $H_x(t)$, $H_y(t)$, $H_z(t)$.

After sophisticated signal analysis, these are transformed into corresponding electric and magnetic frequency spectra, i.e. $E_x(t) \leftrightarrow \tilde{E}_x(f)$

We then form estimates of the MT *Impedance tensor* (or "EMTF") **Z**, a complex-valued 4 x 4 tensor defined at a set of discrete frequencies – each representing a different depth of penetration sampling a different volume average of the subsurface.

We also form estimates of the MT *Induction vector* (or "Tipper") T, the ratio of vertical to horizontal magnetic field components.

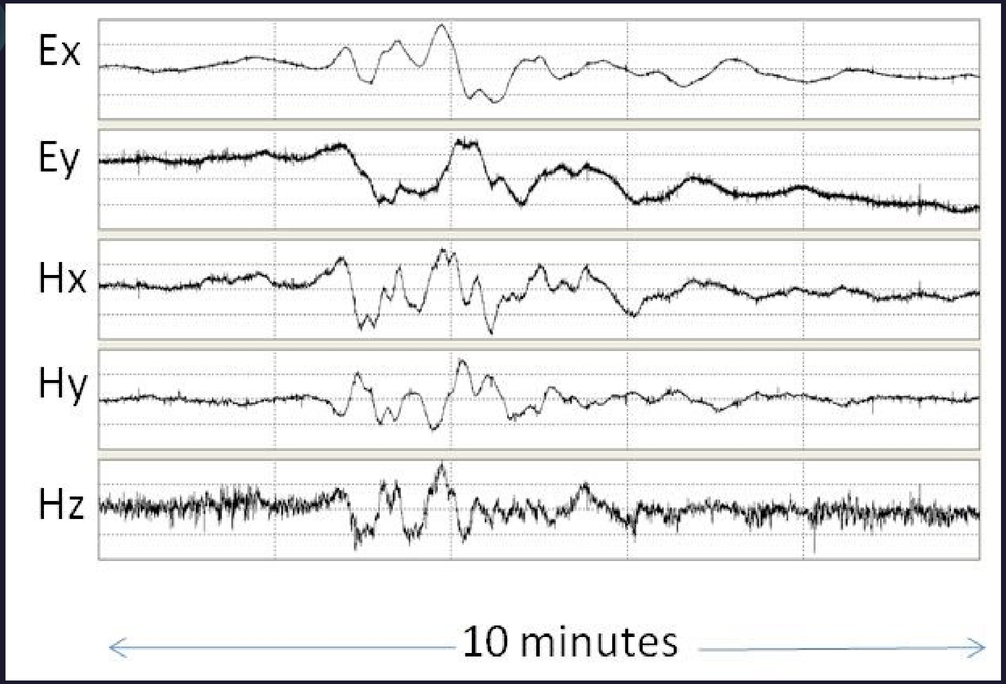


$$\begin{bmatrix} E_x \\ E_y \end{bmatrix} = \begin{bmatrix} Z_{xx} & Z_{xy} \\ Z_{yx} & Z_{yy} \end{bmatrix} \begin{bmatrix} H_x \\ H_y \end{bmatrix} + U,$$

$$H_z = \begin{bmatrix} H_x & H_y \end{bmatrix} \begin{bmatrix} T_x \\ T_y \end{bmatrix} + U.$$

# Magnetotelluric response functions in human-readable form

Each element of the complex-valued impedance tensor can be transformed into real-valued *apparent resistivity and phase.* $\rho_a$ is simply the scaled magnitude of the impedance while $\Phi$ is the phase, i.e. the amount by which the electric field at a given frequency lags or leads the magnetic field in time. If $\Phi > 45^o$ this indicates that the resistivity structure is getting more conductive at whatever depth corresponds to that frequency, and if $\Phi < 45^o$, more resistive.

$$\rho_{a,xy}(T) = \frac{T}{2\pi\mu_0}\left\lfloor Z_{xy}\right\rfloor^2, \qquad \phi_{xy} = \arctan(\frac{Im(Z_{xy})}{Re(Z_{xy})})$$

- If the resistivity varies only with depth (1-D), the relationship between E and H doesn't depend on azimuth, so the impedance tensor reduces to Zxy = -Zyx, Zxx=Zyy=0.
- For 2-D resistivity structure, Zxy and Zyx are defined and their magnitudes are not equal; Zxx=Zyy=0.
- For 3-D resistivity structure, all elements of the impedance tensor are non-zero.

# The Magnetotelluric Method (MT)

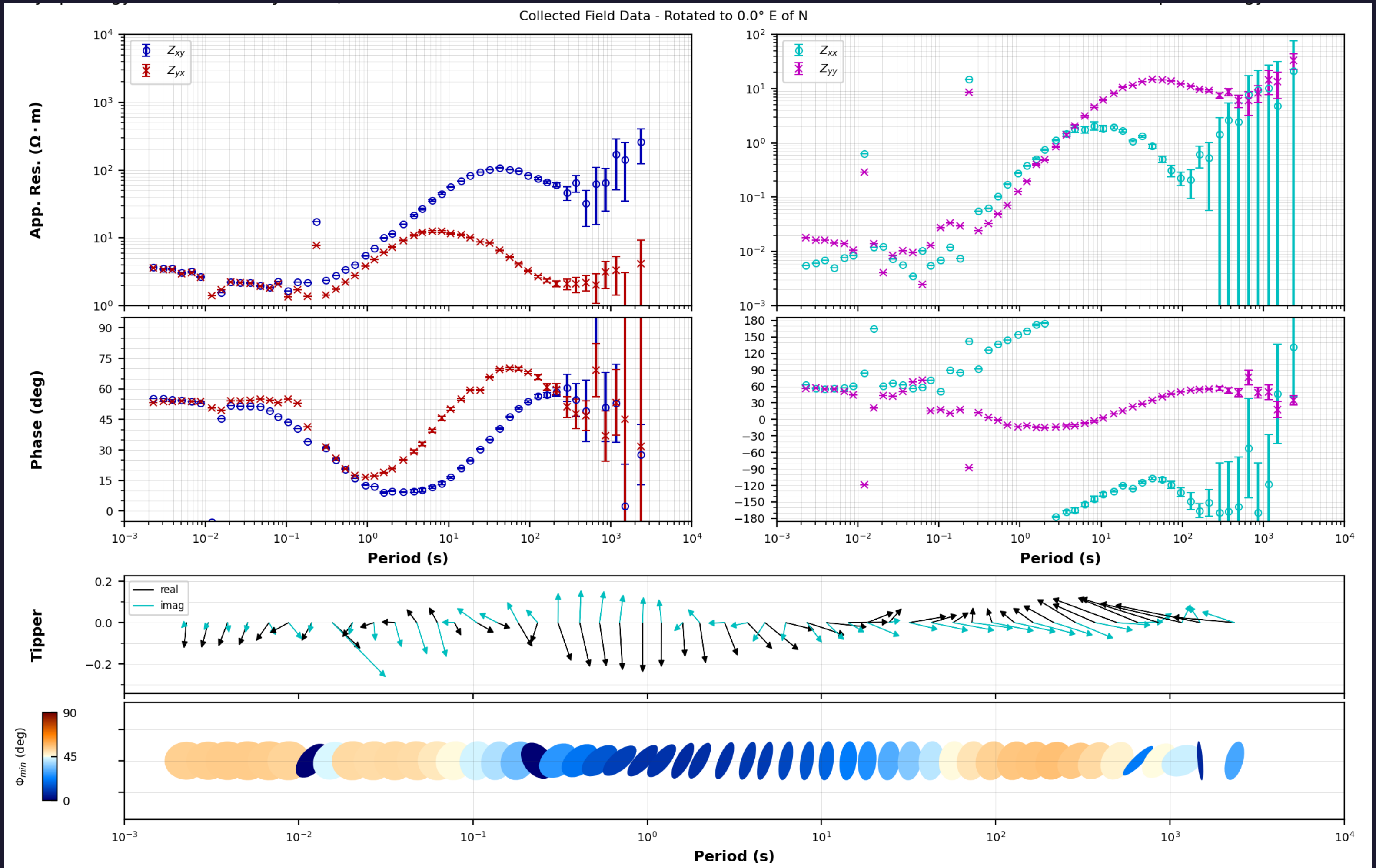


Example of apparent resistivity, phase, tipper and phase tensor data from a commercial wideband MT survey in the Great Basin of the western US.

The four complex-valued elements of the impedance tensor at each period $Z_{xx}$, $Z_{xy}$, $Z_{yx}$, and $Z_{yy}$ are transformed into the four real-valued elements of apparent resistivity and phase in the top two columns and rows of the figure.

Below this is the real and complex values of the induction vector (Tipper) – the ratio of the vertical magnetic field to the horizontal magnetic field components.

# The Magnetotelluric Method (MT)

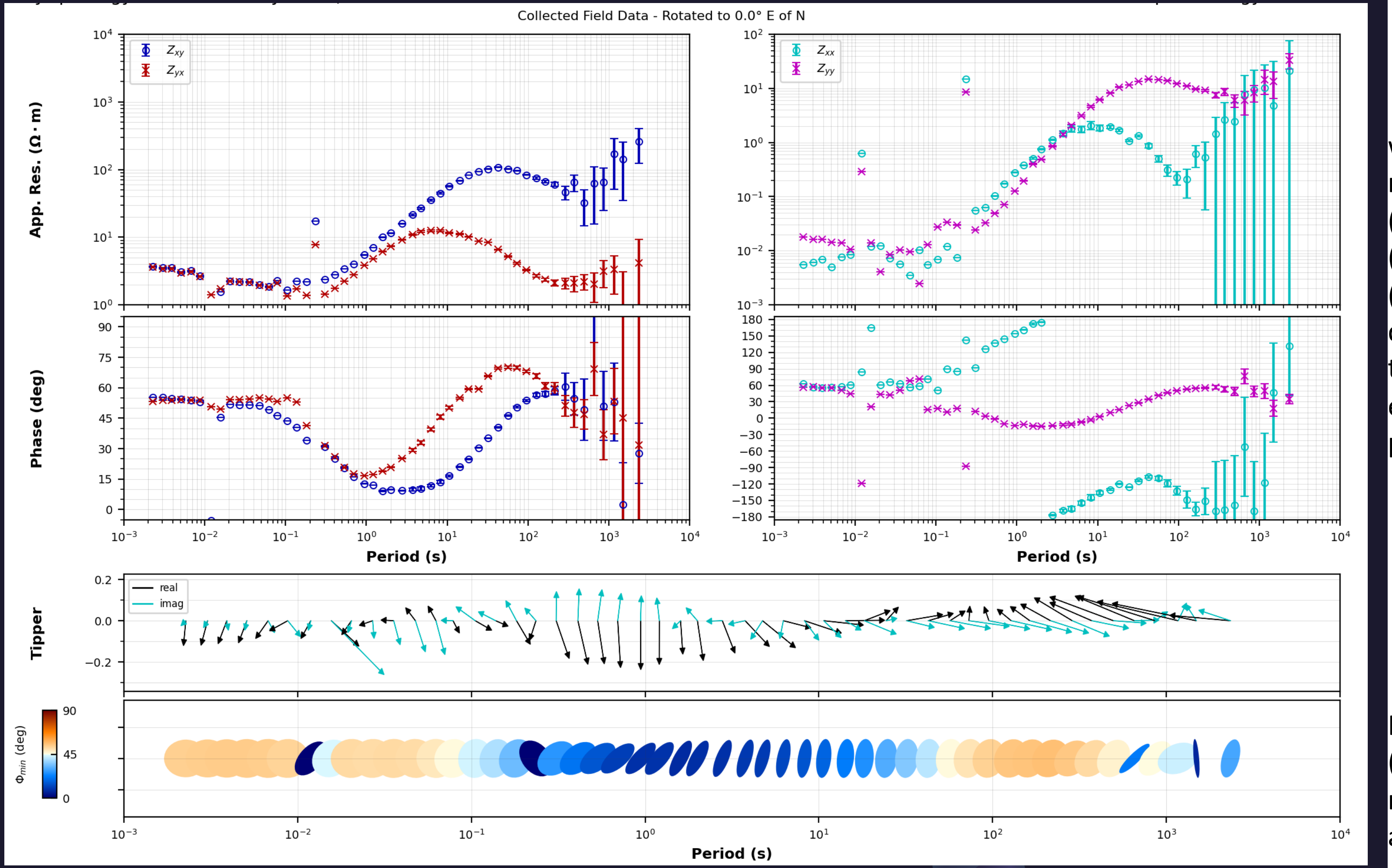


The MT phase tensor is written as:

$$\Phi = Re(\mathbf{Z})^{-1} Im(\mathbf{Z}) = \begin{bmatrix} \Phi_{xx} & \Phi_{xy} \\ \Phi_{yx} & \Phi_{yy} \end{bmatrix}, \tag{2}$$

where *Re* and *Im* are the real and imaginary components, respectively, of the impedance tensor **Z**. The ellipticity (Φmax and Φmin) of the phase tensor and its skew angle (β) are invariant parameters, insensitive to near-surface (galvanic) distortion effects, that can be used to determine the dimensionality of the regional impedance tensor as well as the direction of geoelectric strike (it is exists). Parameters α and β are calculated from the phase tensor elements:

$$\alpha = \frac{1}{2} arctan\left(\frac{\Phi_{xy}+\Phi_{yx}}{\Phi_{xx}-\Phi_{yy}}\right), \tag{3}$$

$$\beta = \frac{1}{2} arctan\left(\frac{\Phi_{xy}-\Phi_{yx}}{\Phi_{xx}+\Phi_{yy}}\right). \tag{4}$$

If the regional resistivity structure is 1-D, Φmax = Φmin (i.e. a defining a circle rather than an ellipse), and if the regional structure is 2-D, Φmax ≠ Φmin, β=0 and α is the azimuthal angle of the major axis of the phase tensor ellipse. The geoelectric strike direction (defined for 2-D

# The Magnetotelluric Method (MT)
# Long-Period MT in Cascadia

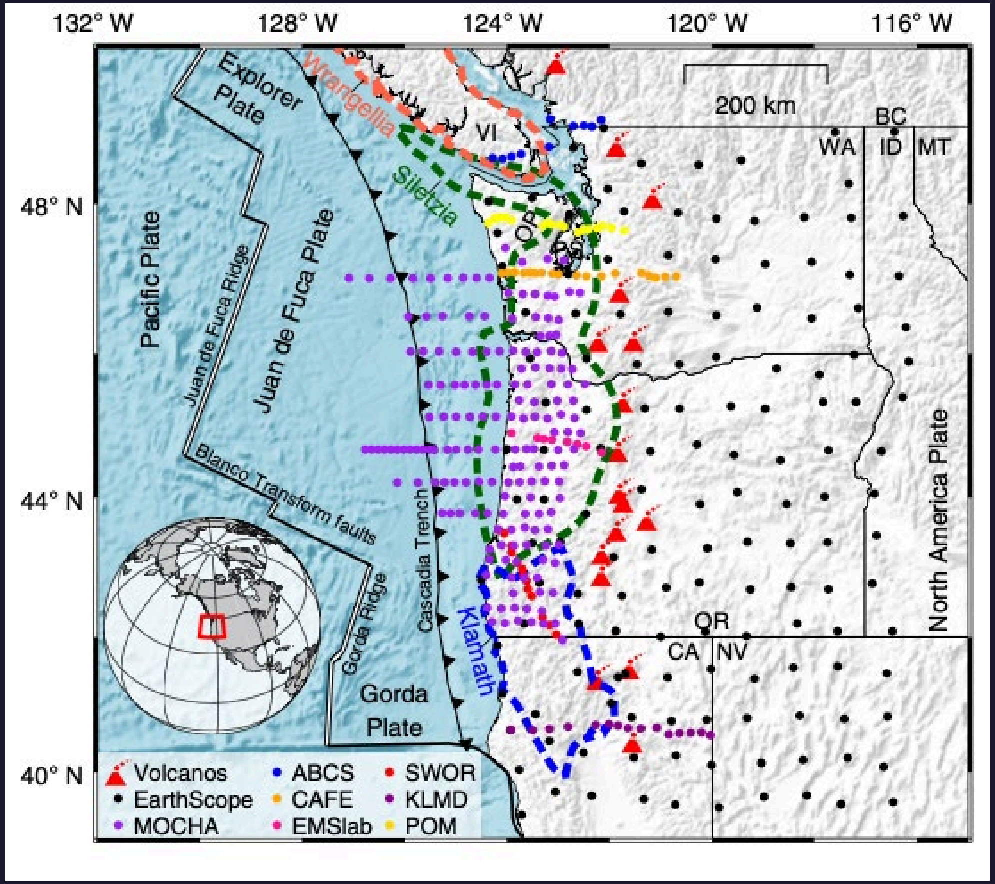


nature geoscience
Received: 29 April 2021; Accepted: 30 May 2022;
Published online: 14 July 2022
ARTICLES
https://doi.org/10.1038/s41561-022-00981-8
Check for updates

## Fluid transport and storage in the Cascadia forearc influenced by overriding plate lithology

Gary D. Egbert[1], Bo Yang[2]✉, Paul A. Bedrosian[3], Kerry Key[4], Dean W. Livelybrooks[5], Adam Schultz[1,6], Anna Kelbert[7] and Blake Parris[5]

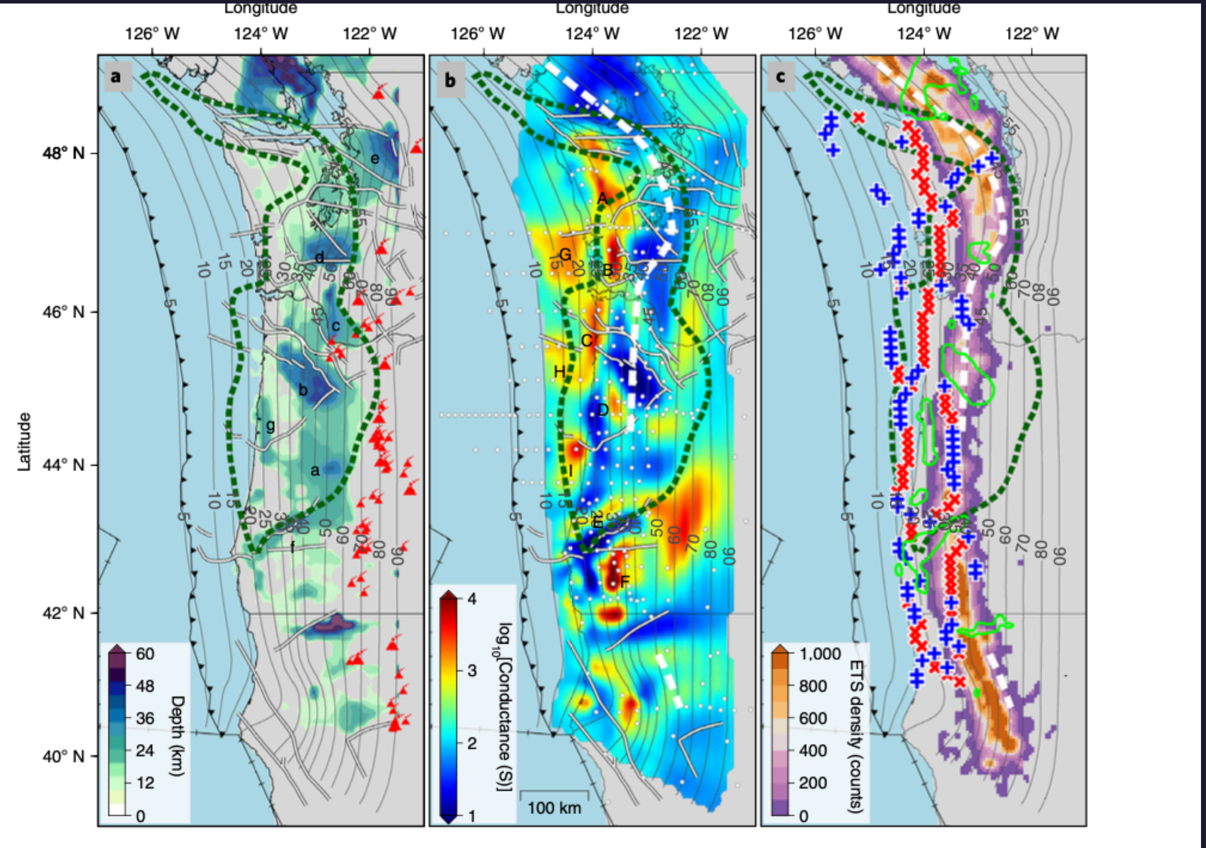


**Fig. 3 | 2D views derived from the 3D resistivity model.** Slab depth contours[61] are plotted as thin black lines, and the outline of Siletzia[36] is shown by the green dashed line. **a**, Depth to the bottom of the 300 Ω m isosurface. The crustal column between this depth and ~5 km depth is almost always at least 300 Ω m (Fig. 2 and Supplementary Fig. 1). Crustal faults[18] are shown by white lines and volcanic vents[62] are marked by red symbols. The resistive blocks discussed in text are labelled a–g. **b**, Conductance of the 10 km layer above the plate interface. Magnetotelluric sites are shown by small white circles, and conductive features discussed in the text are labelled A–I. **c**, The positions of highest (red crosses) and second highest (blue crosses) conductance peaks as a function of latitude are plotted over the ETS density for 2009–2019 (ref. [63]). Patches where resistive material extends to the plate interface (from **a**) are outlined in green and the estimated position of the FMC[49] is shown by the thick white dashed line.

# The MOCHA Project

The magnetotelluric (MT) method determines the subsurface resistivity structure from observations of time-varying electromagnetic fields at the earth's surface. It is **directly sensitive** to conductive materials, including brines in subduction zones.

The MOCHA project imaged a conductive band correlating with ETS activity at Cascadia subduction zone.

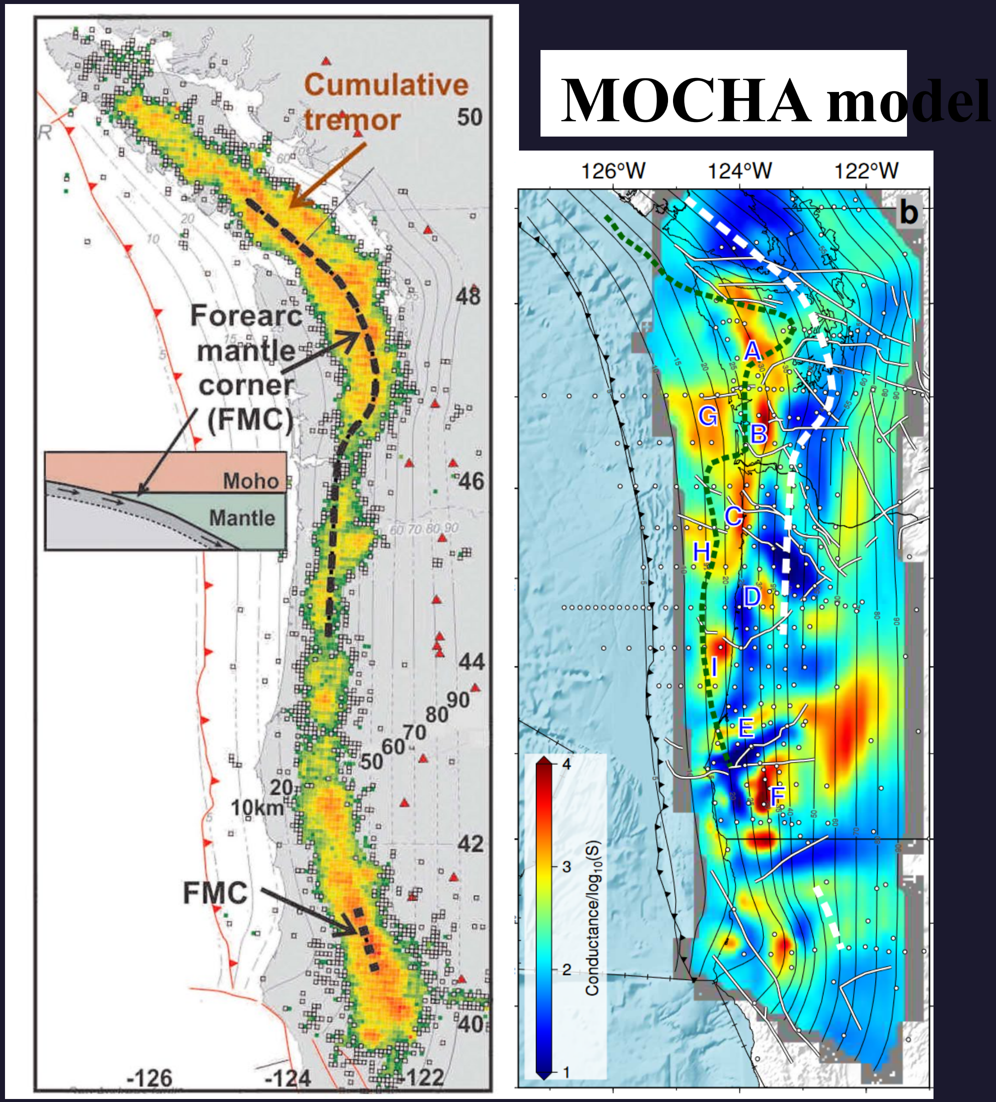


Maps of ETS events (Hyndman et al., 2015) and imaged fluid distributions with MT (Egbert et al., 2022)

# MOCHA provides a snapshot in time reference model

ETS density for 2009–2019 overlayed on a resistivity map at depth of 35 km.

White solid lines enclose areas with more than 80 registered ETS events during 2009-2019.

The MOCHA model provides a **baseline reference model** for continuous MT monitoring of the system over the time-scale of ETS cycles.

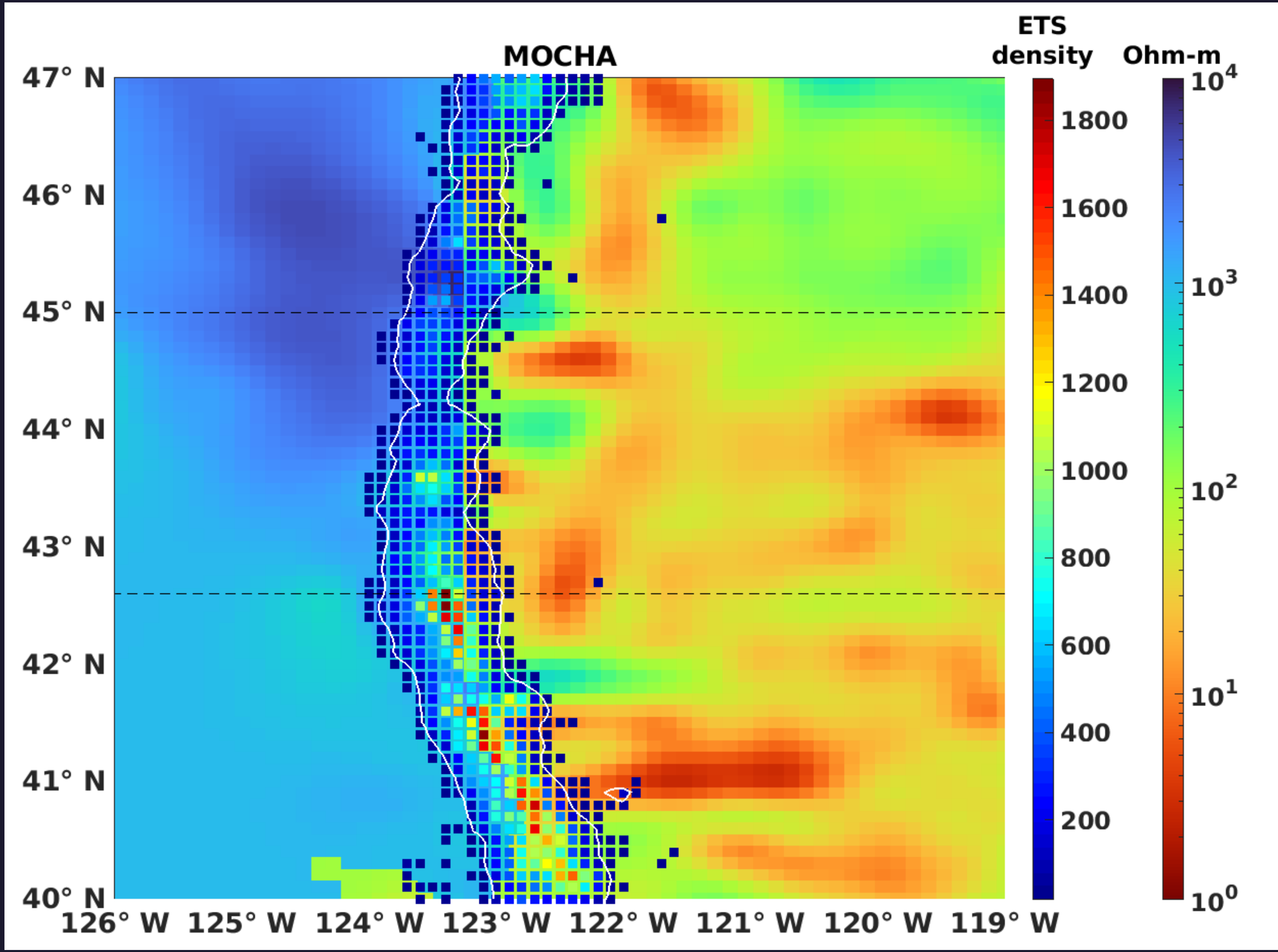

# ..The MOCHA Model

Vertical sections:

Latitude: 45.0ºN

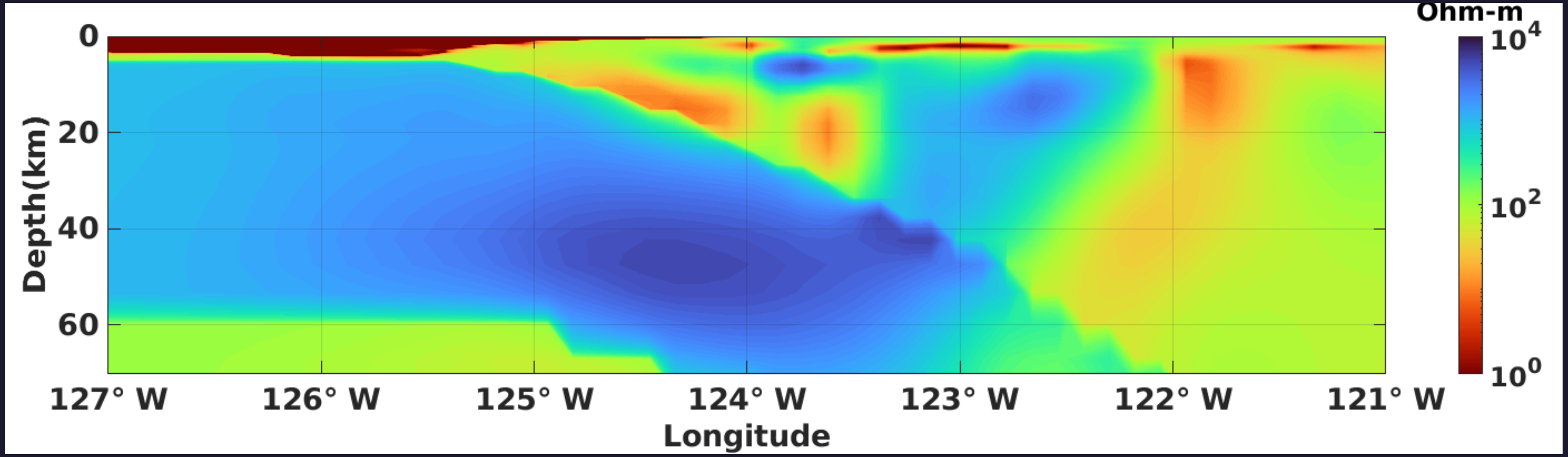


Latitude: 42.6ºN

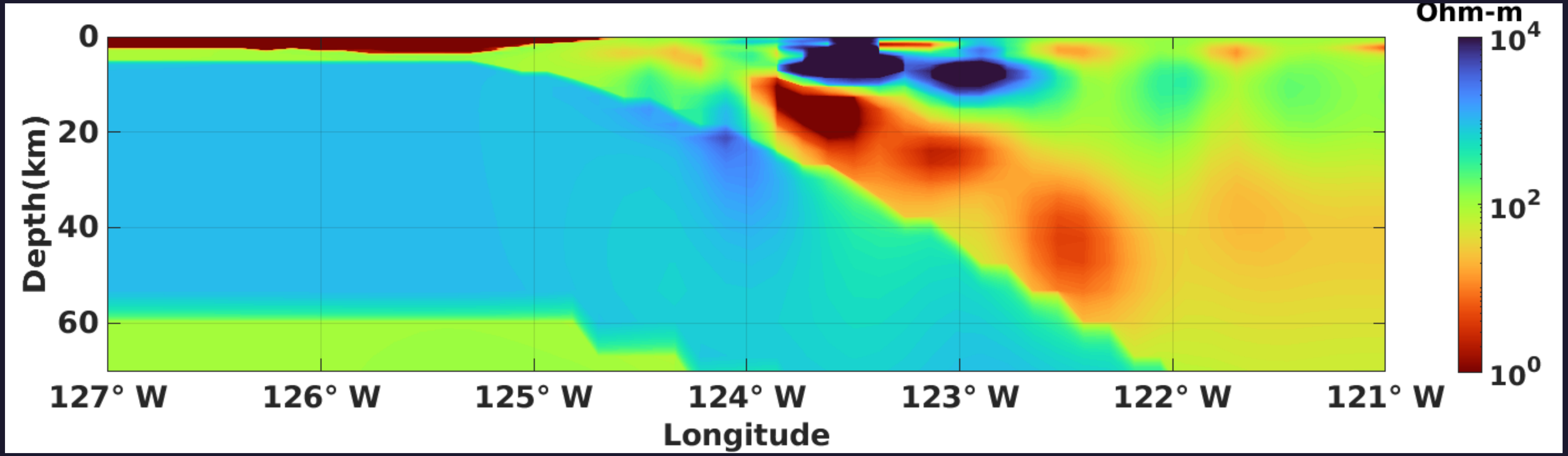

# Continuous MT monitoring

We investigate the **feasibility** of MT to monitor the **cyclic release and migration** of slab-derived fluids associated with ETS.

Can fluid- release and migration associated with ETS produce detectable MT signals at the surface?

Designed MT stations on a map of resistivity model at the depth of 35 km

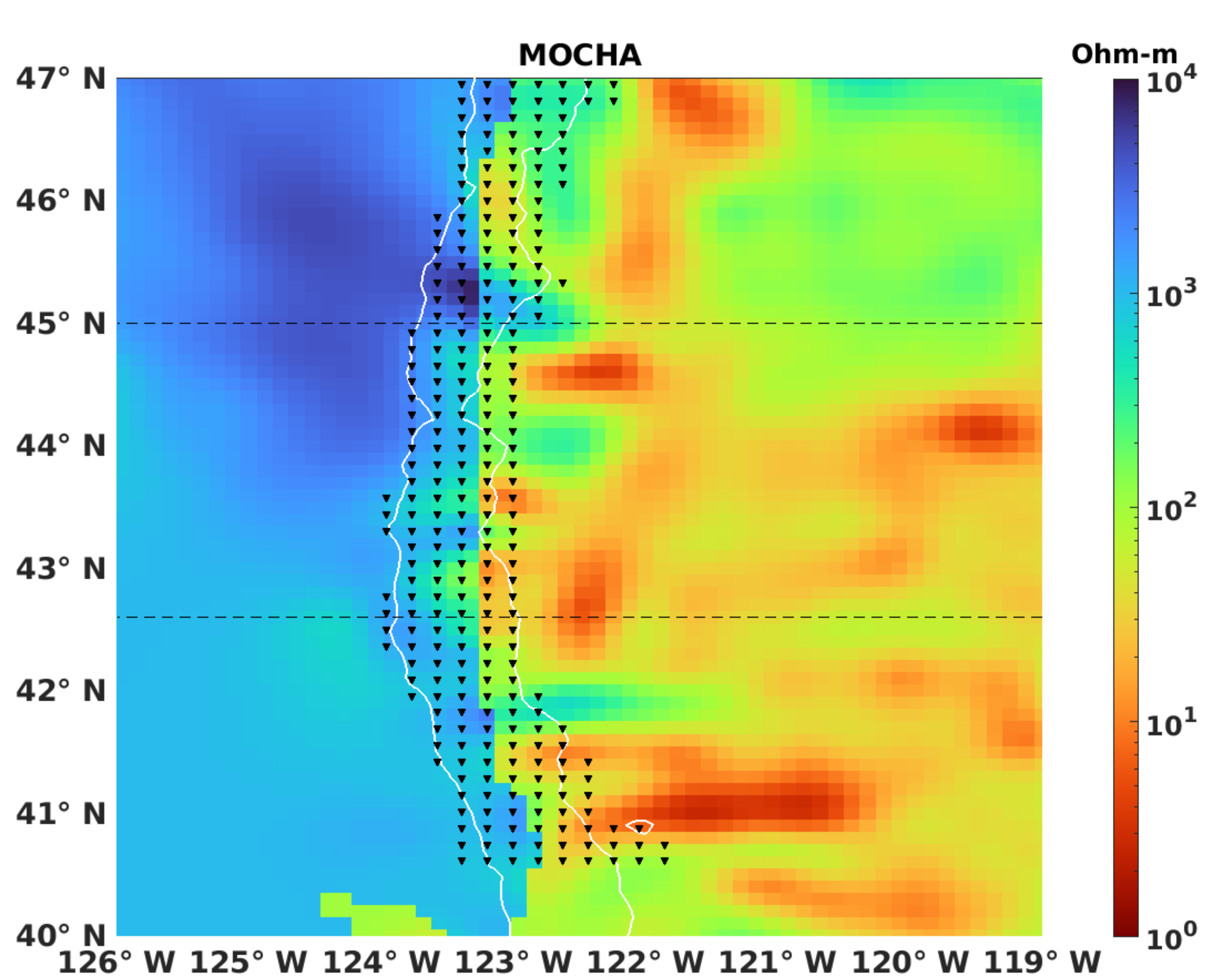

# ETS Zone Thickness

Seismically imaged Slab interface imposed on MOCHA model

Red line: Slab interface

Black line: Top of low velocity zone

White line: bottom of oceanic crust

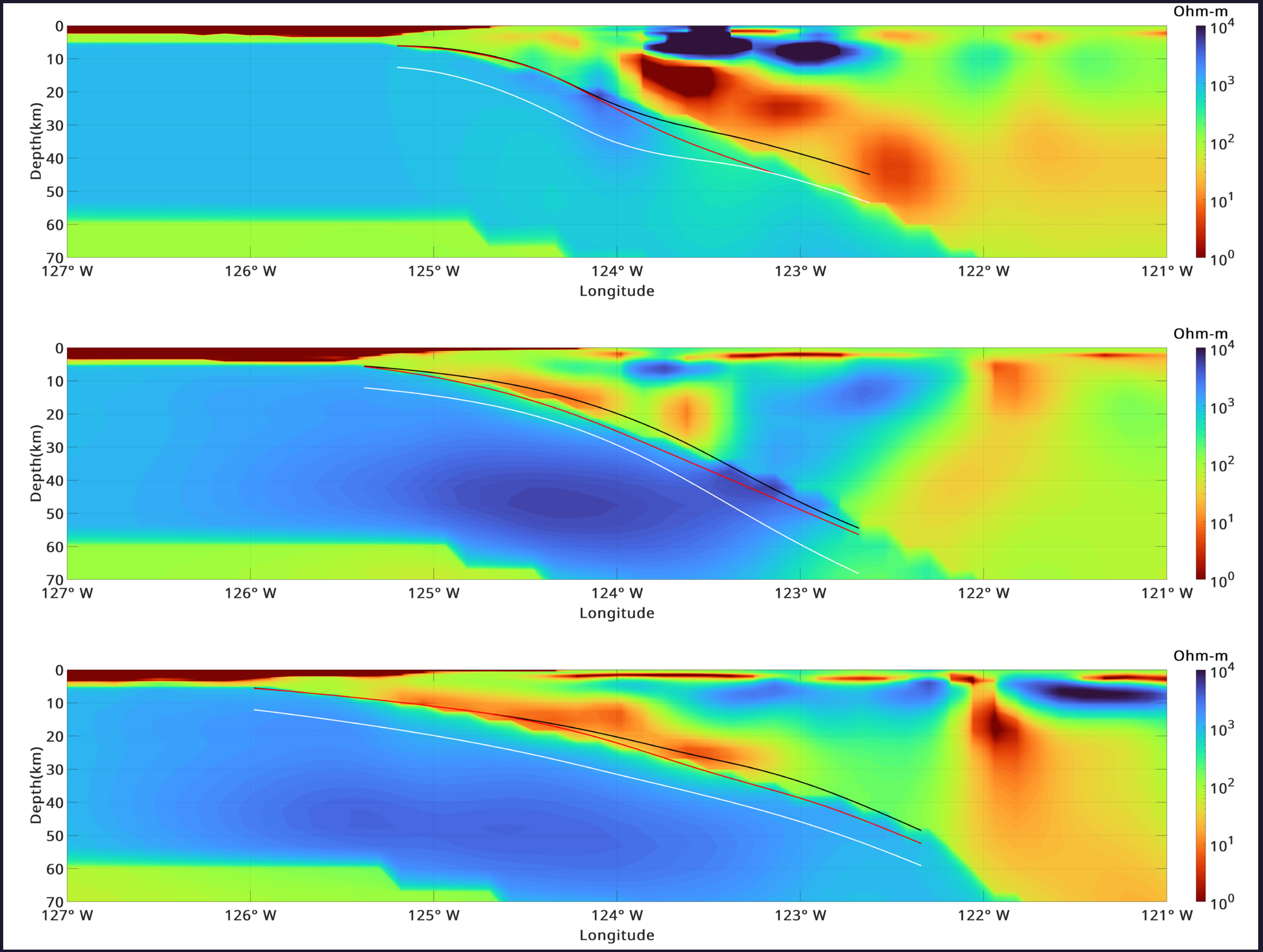

# ETS Zone Porosity

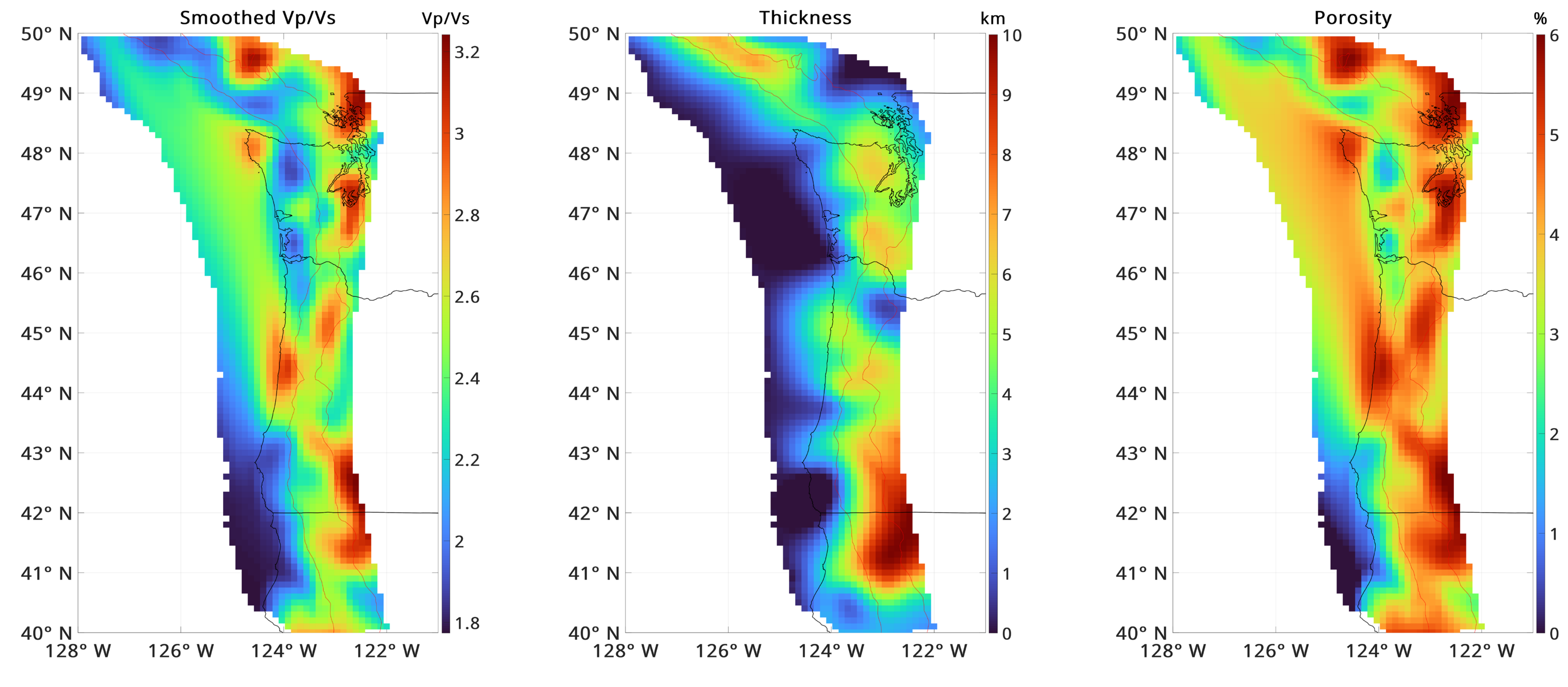


Porosity calculated from Vp/Vs (Bloch et al., 2023) using rock physics model (Peacock et al., 2011)

# ETS Zone Resistivity

ETS zone resistivity as a function of porosity and cementation factor (controlled by permeability) calculated with Archie's law

Resistivity values imaged by MOCHA are bounded by the two white dashed lines

Seismic studies estimated ave. porosity at Cascadia ETS zone as 2.7-4% (Peacock, et al., 2011; Bostock, 2013).

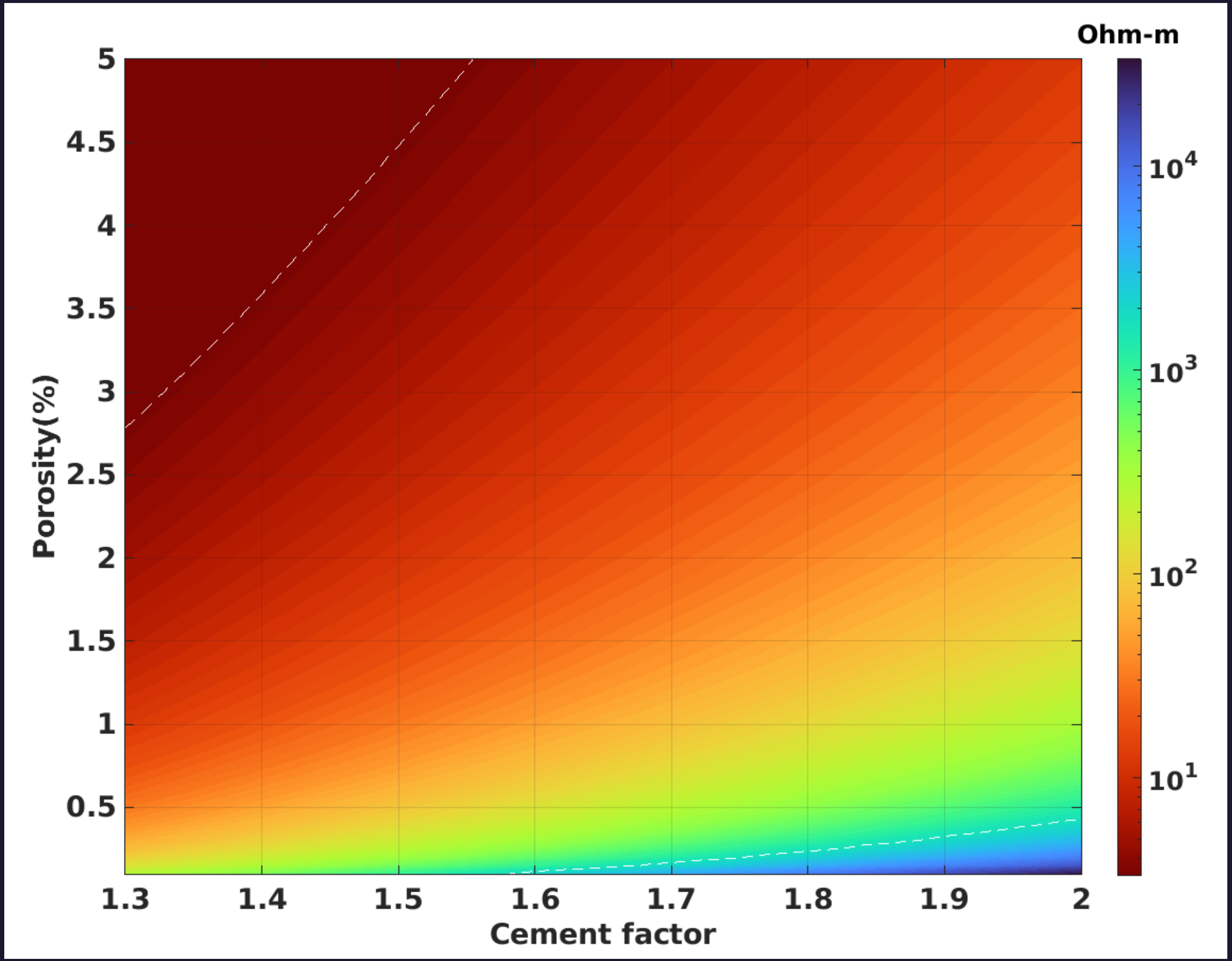

# ..Simulate resistivity variations during ETS cycle

Cementation factor decreased to a constant = 1.5 ~40 km downdip along slab interface

ETS layer thickness and porosity are from seismic model

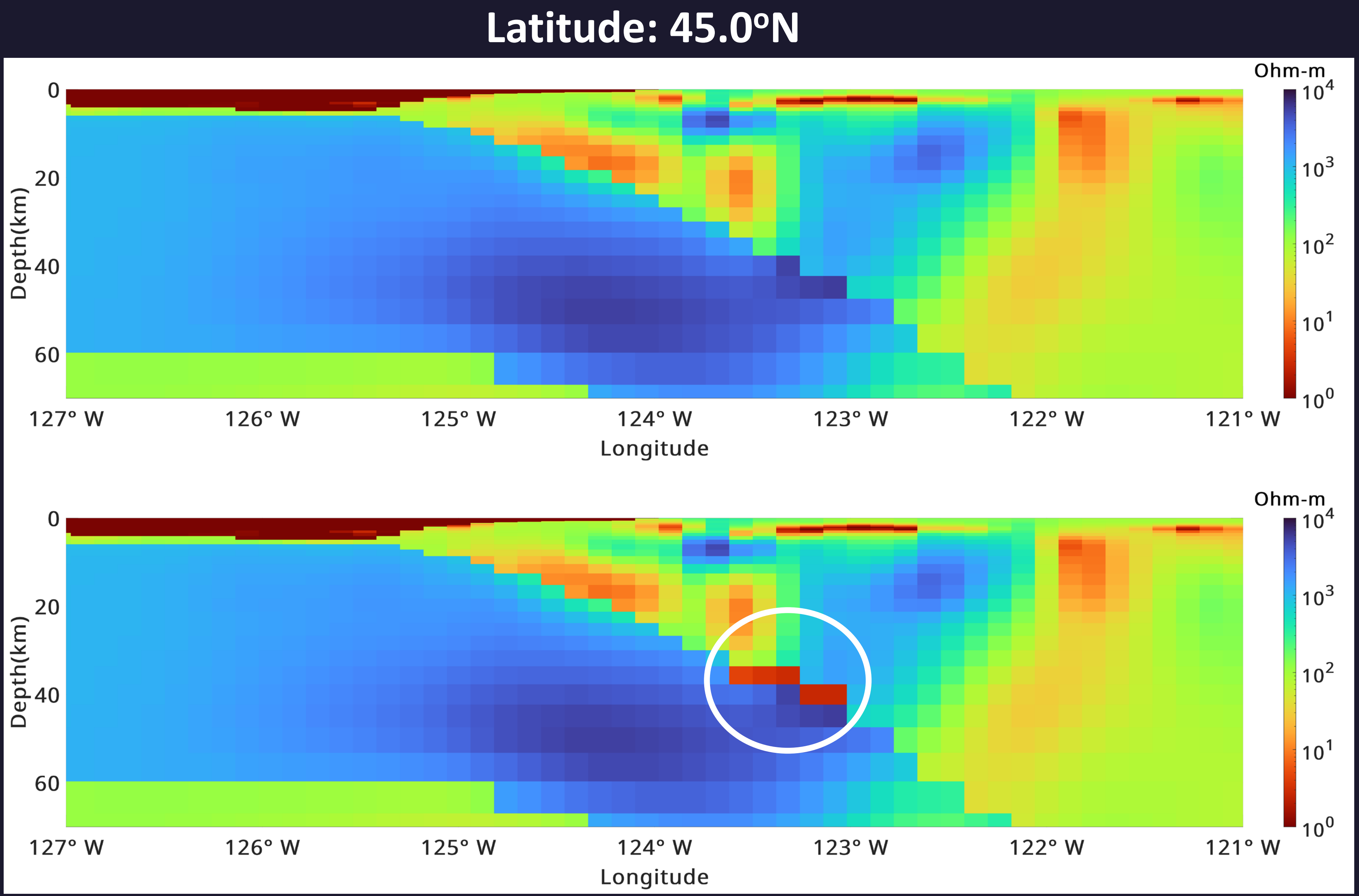

# ..Resistivity Variations

Cementation factor decreased to a constant = 1.5 ~40 km downdip along slab interface

ETS layer thickness and porosity are from seismic model

**Latitude: 42.6ºN**

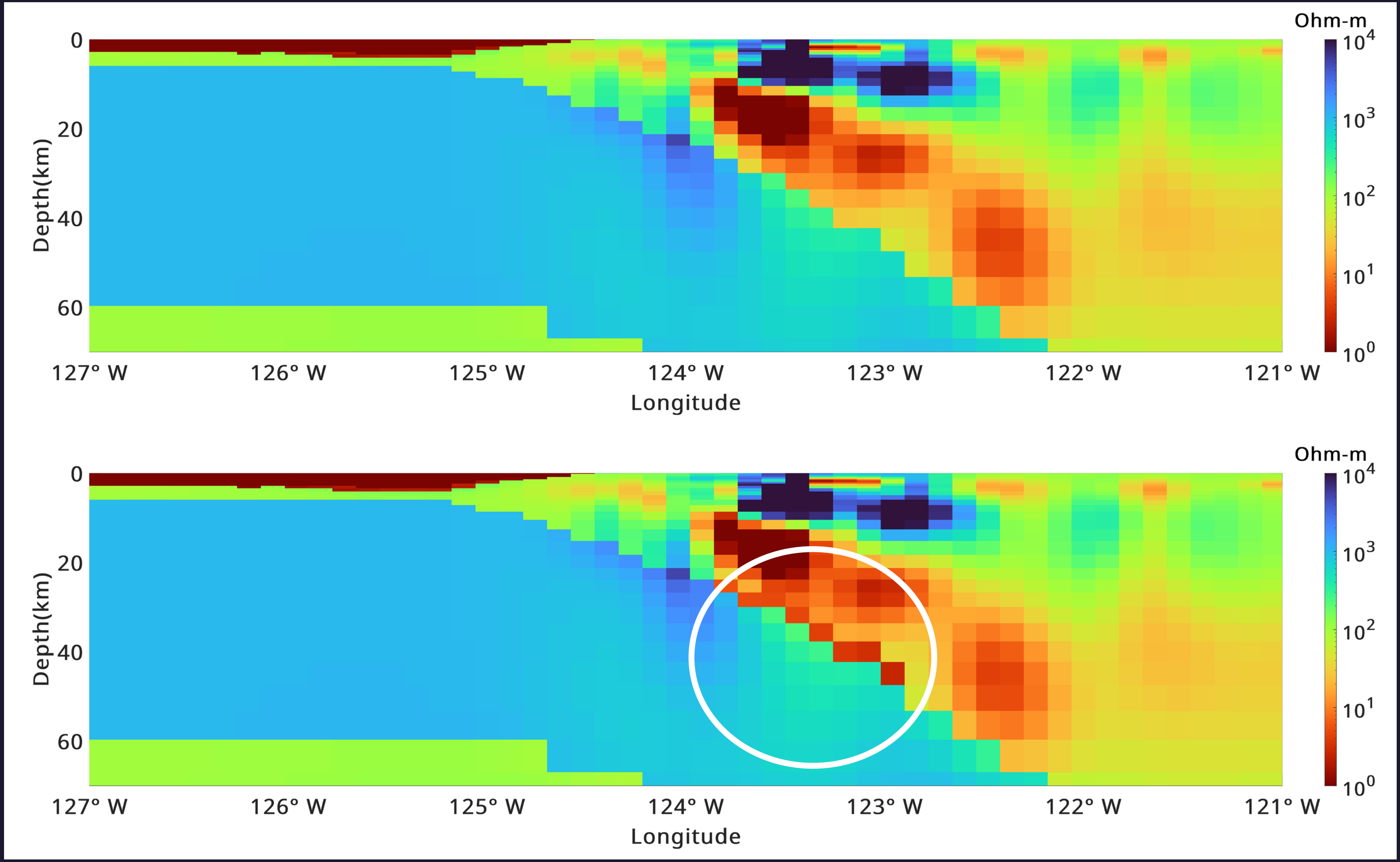

# Resistivity Variations vs. time

Perturbation Model 1 – downdip along entire length of slab interface

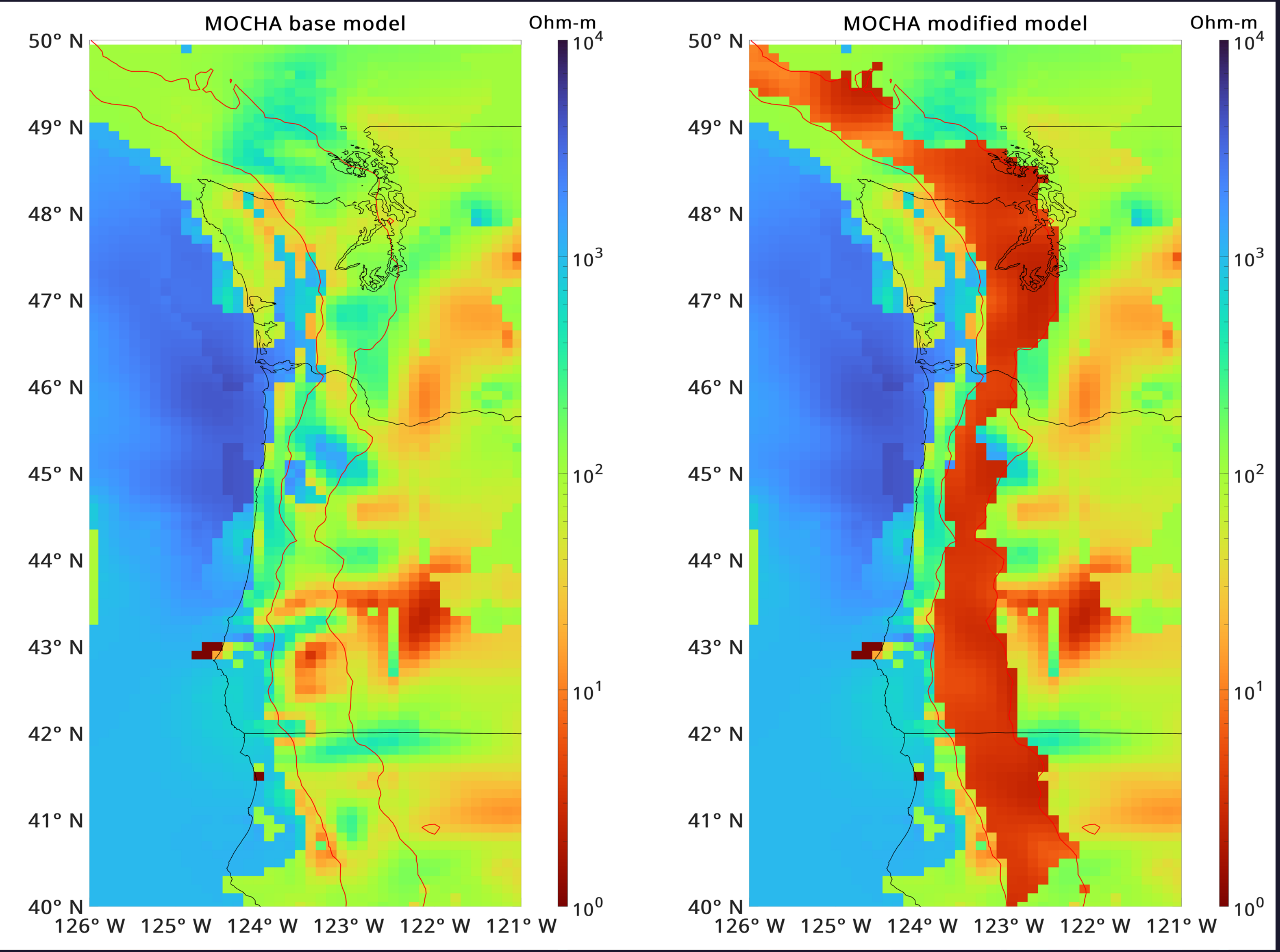

# MT Response: model 1

## Cementation factor: 1.5, change in MT response 41.7°N, 122.8°W

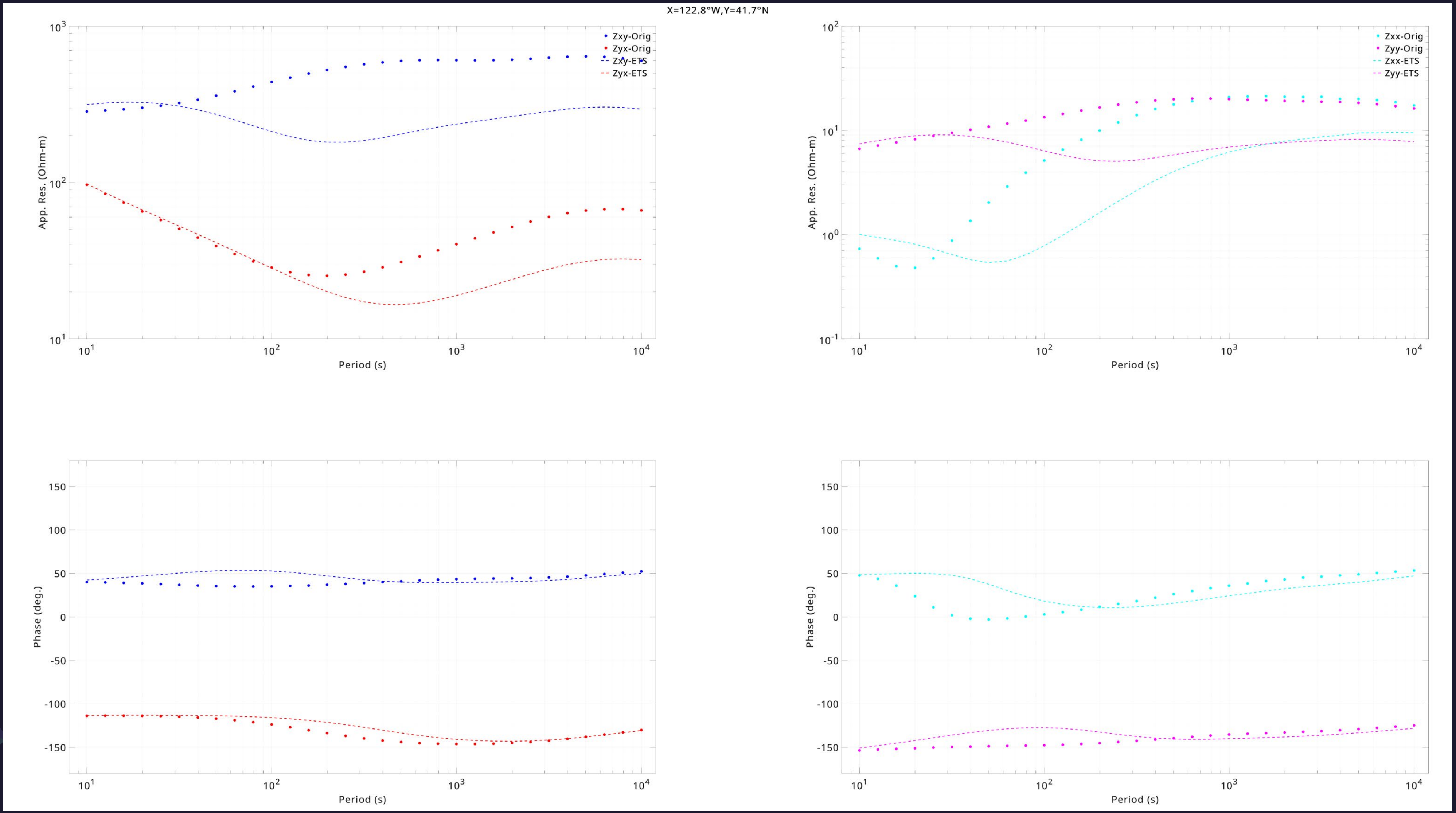

# MT Response: model 1

## Cementation factor: 1.7, change in MT response 41.7°N, 122.8°W

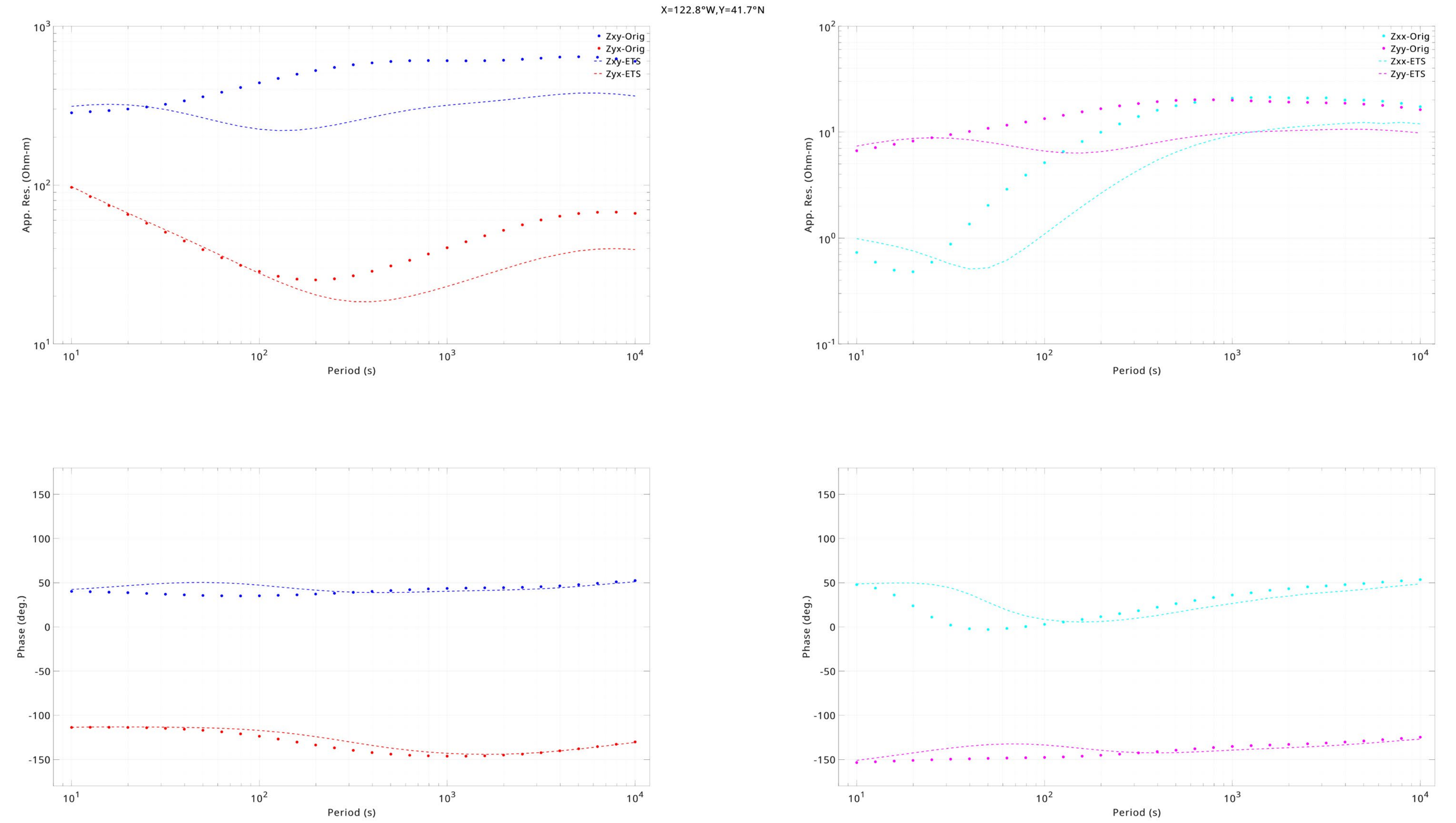

# MT Response: model 1

## Cementation factor: 1.9, change in MT response 41.7ºN, 122.8ºW

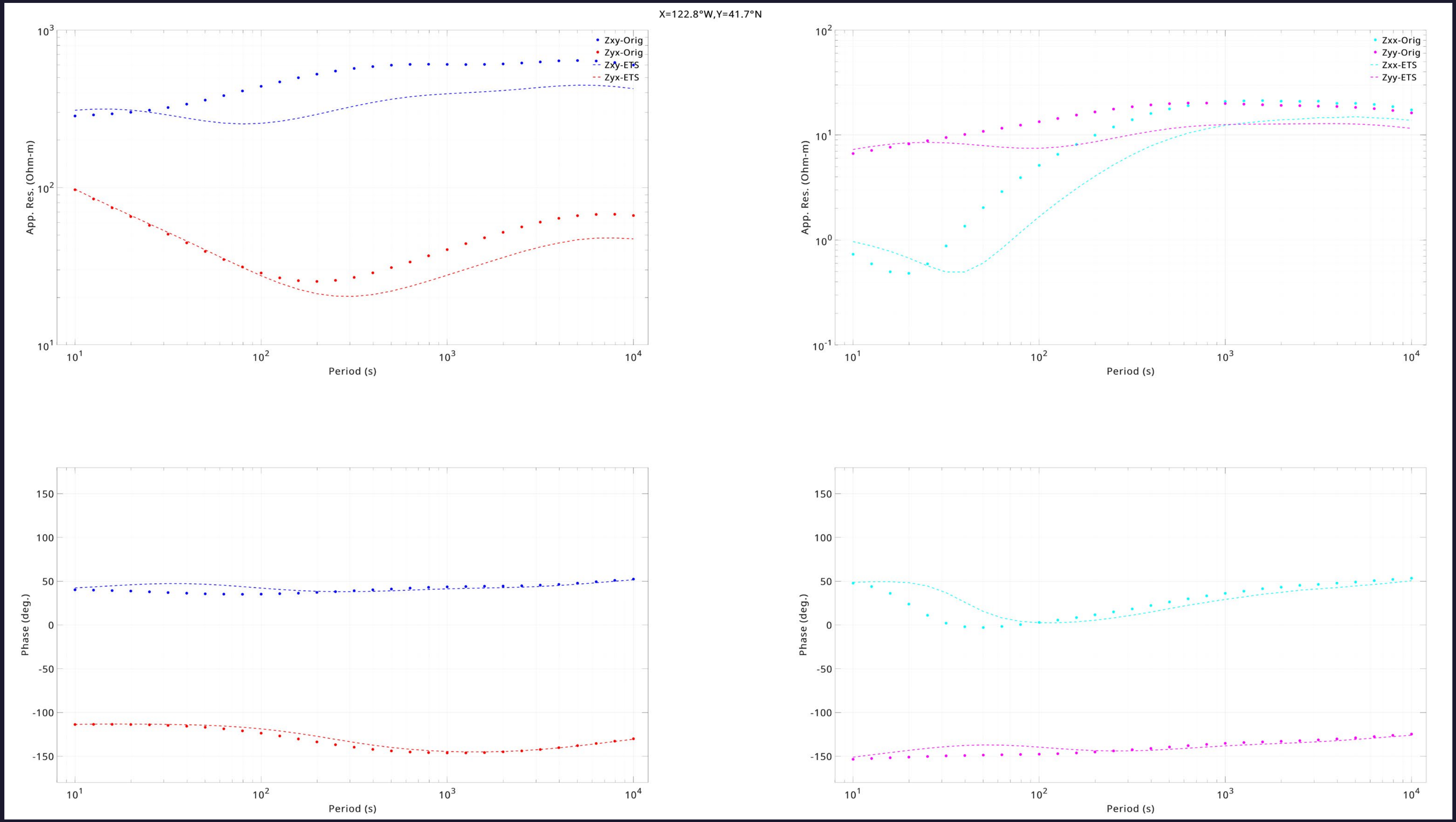

# MT Response: model 1

Cementation factor: 1.5, change in MT response 43.4$^{o}$N, 123.2$^{o}$W

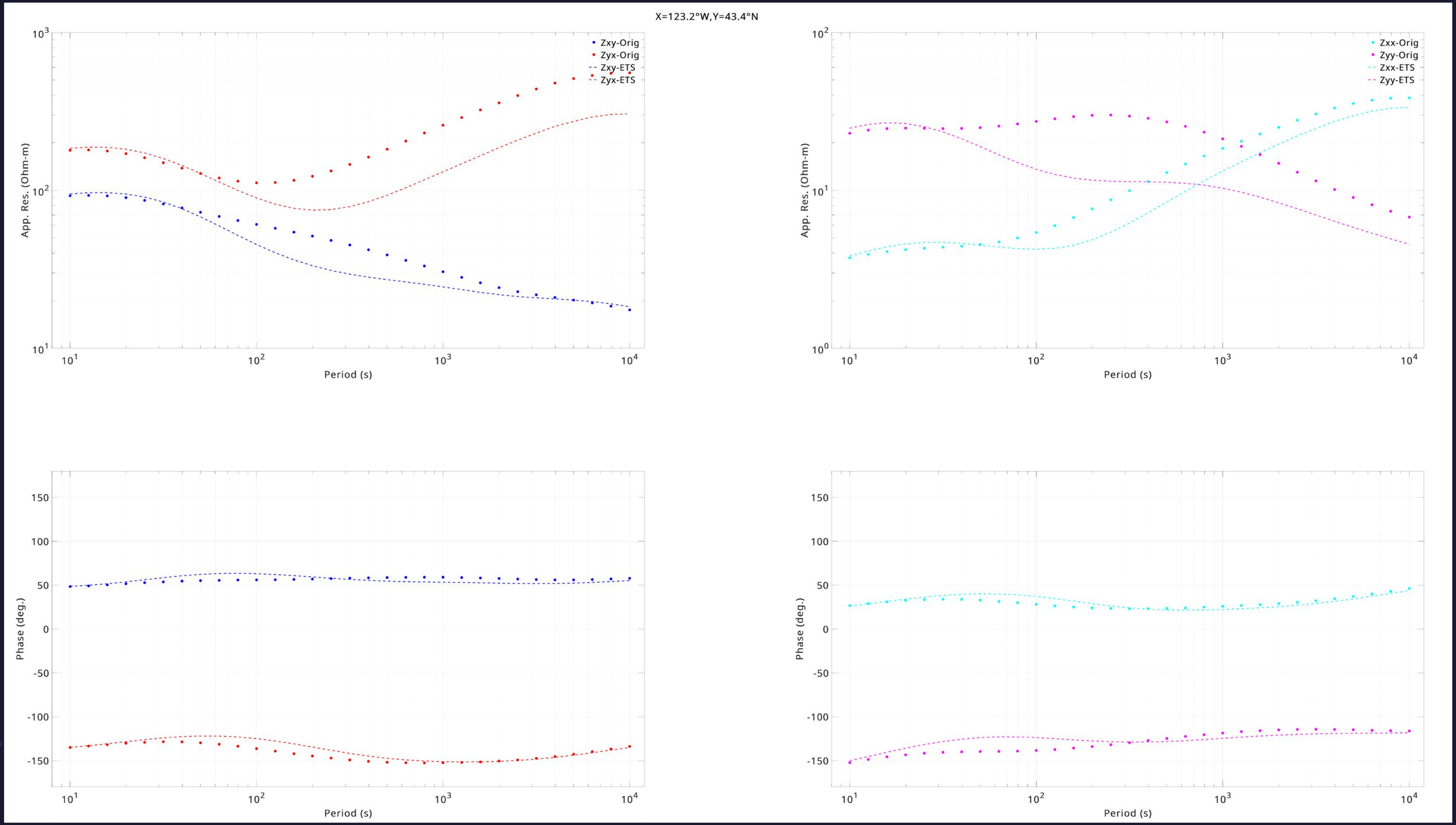

# MT Response: model 1

## Cementation factor: 1.7, change in MT response 43.4°N, 123.2°W

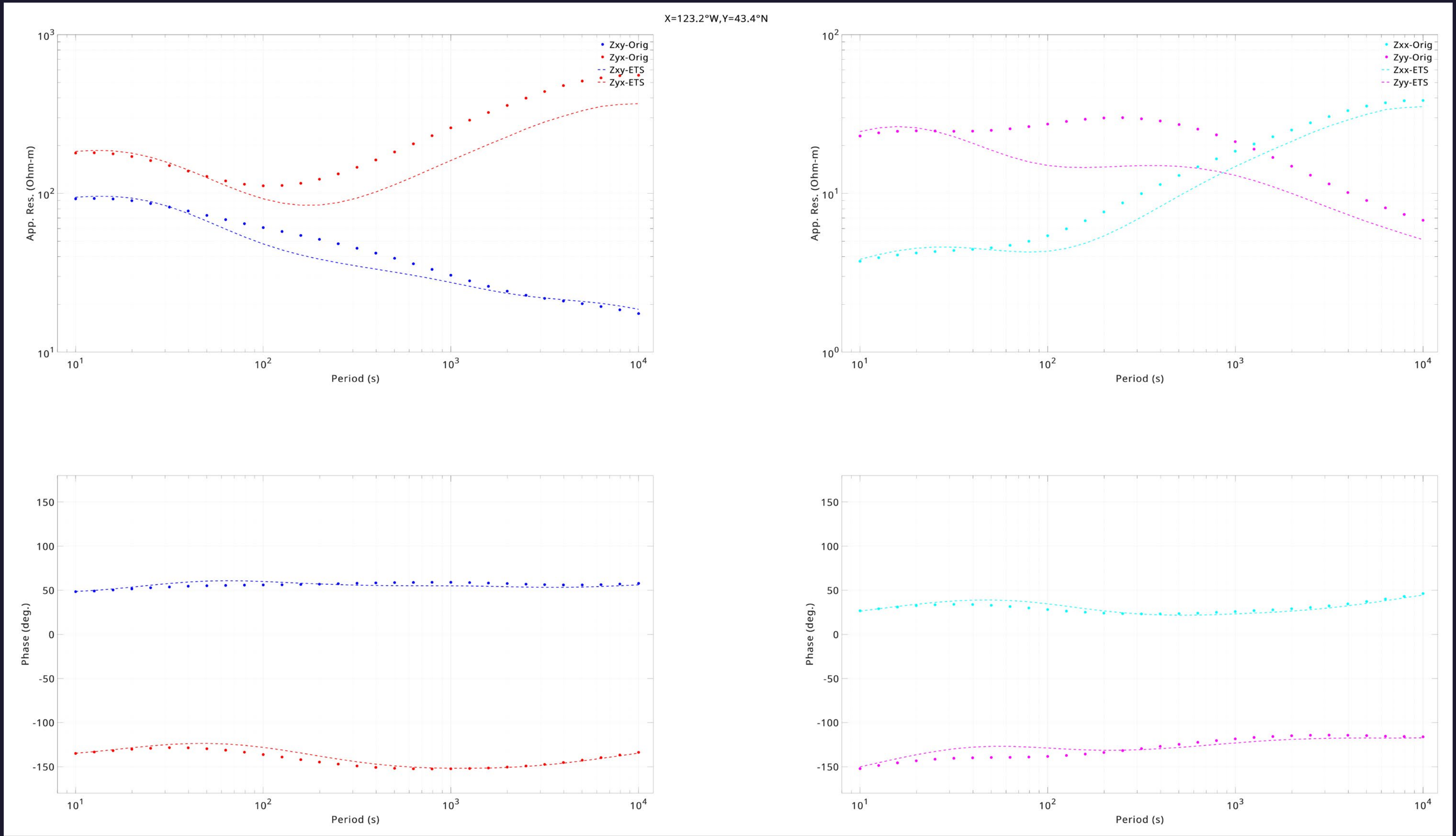

# MT Response: model 1

## Cementation factor: 1.9, change in MT response 43.4°N, 123.2°W

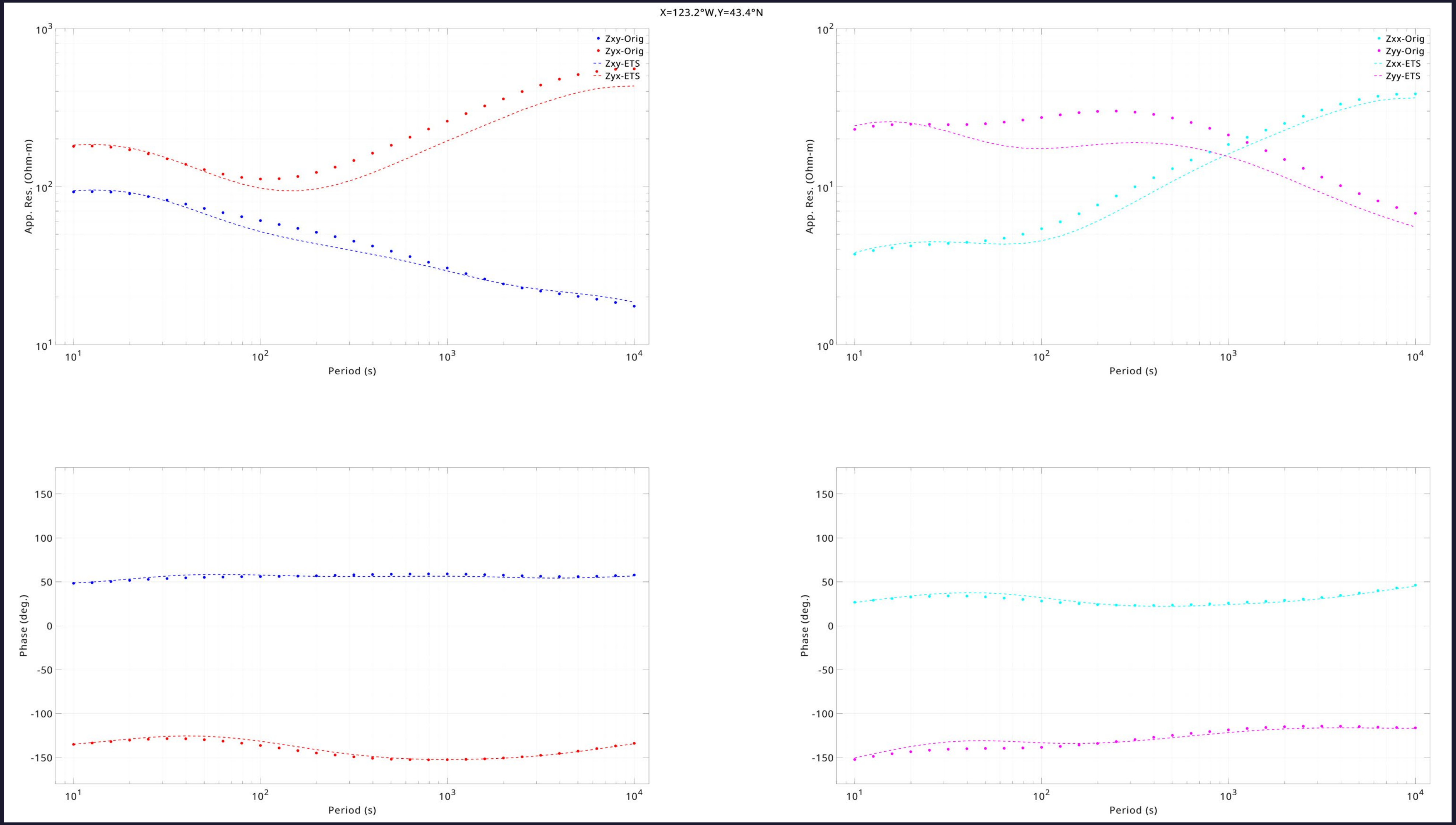

# App. Resistivity Difference: model 1,change in response at 10 s and 25 s period (“detectible if $\Delta\rho_a$ > 3-5%”)

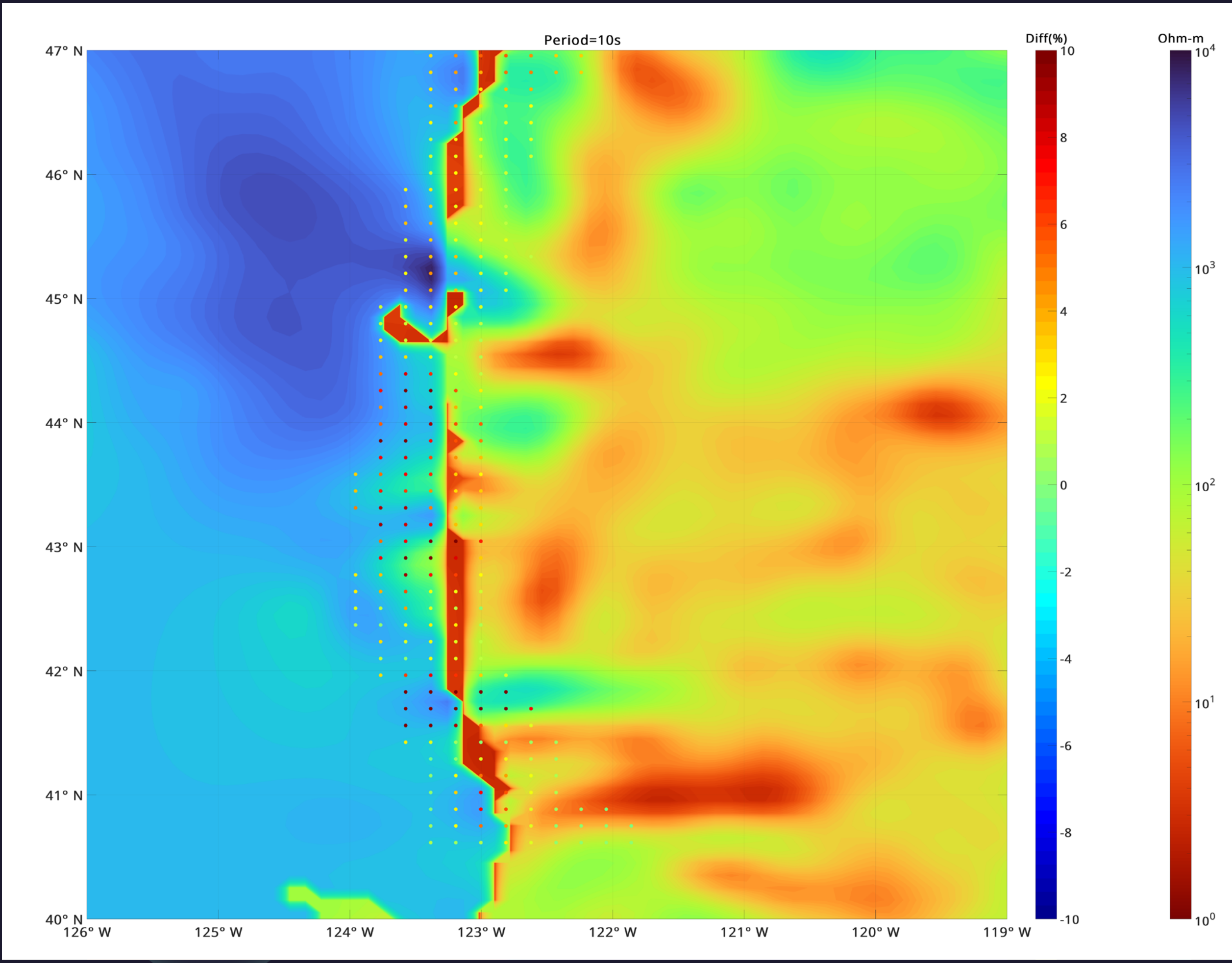


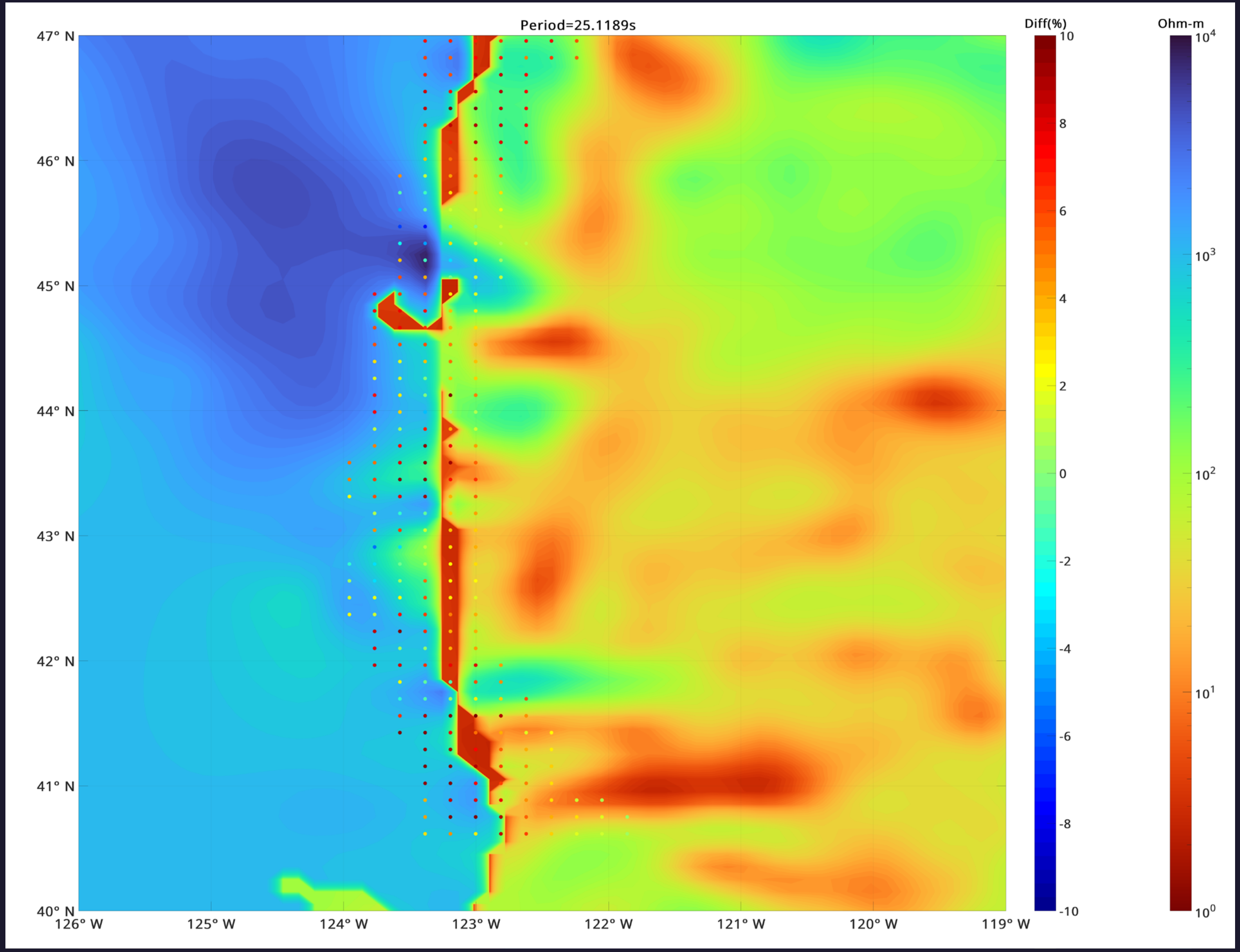


Period (s) of MT response functions scales to depth beneath the surface. Background image is resistivity model at 35 km depth.

# Max. Phase Tensor Difference in Degrees: model 1,change in response at 10 s and 25 s period (“detectible if $\Delta\vartheta > 3\text{-}5^o$”)

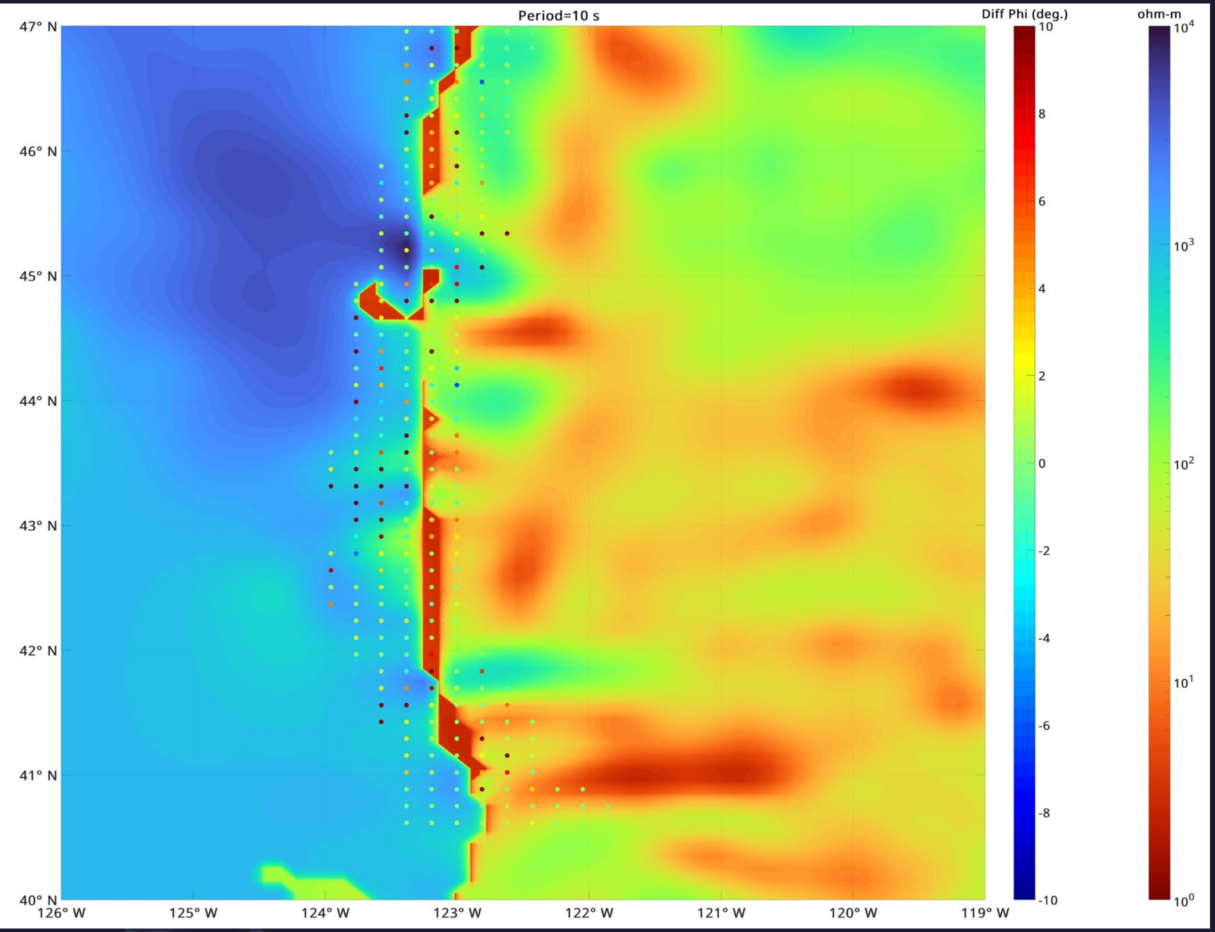


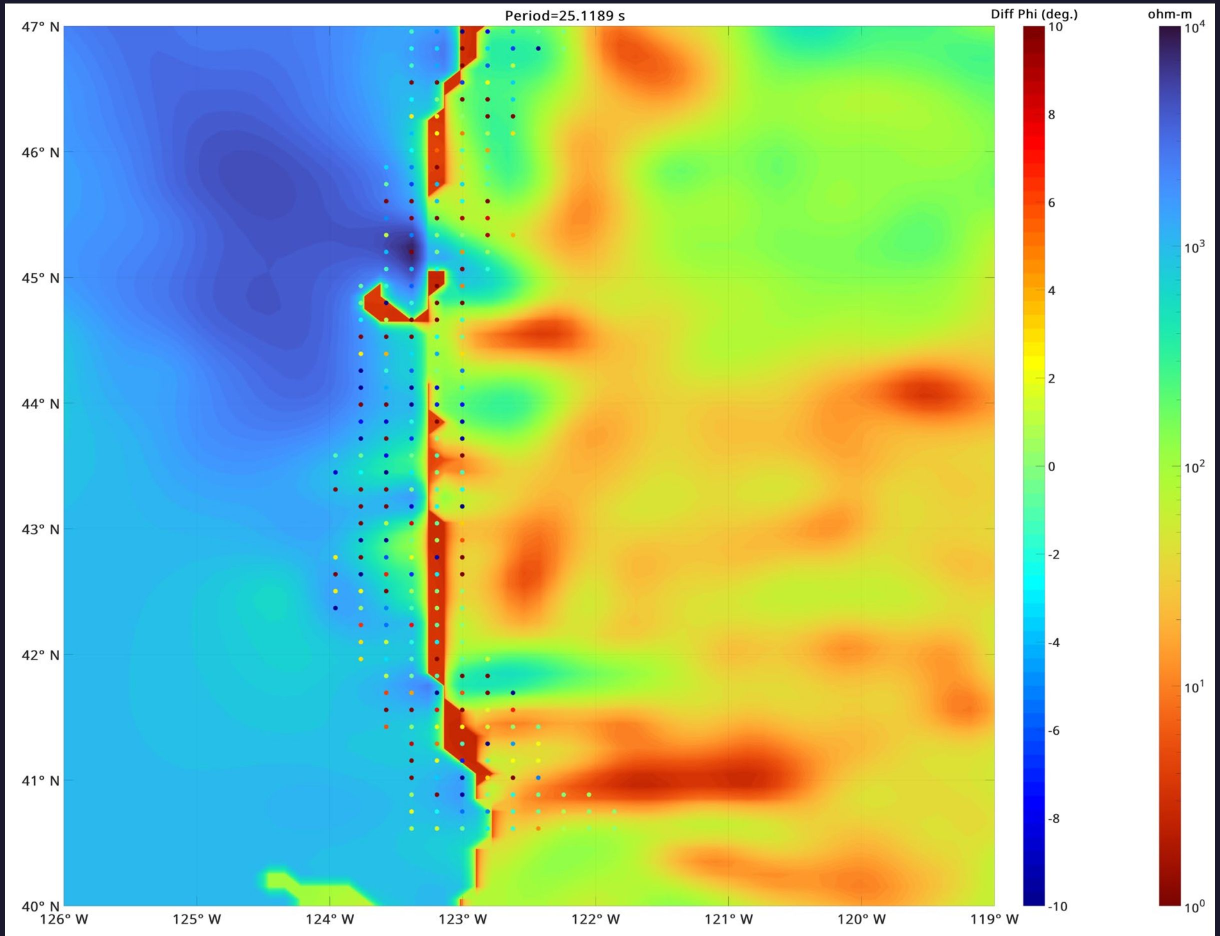

# App. Resistivity Difference: model 1,change in response at 63 s and 158 s period (“detectible if $\Delta\rho_a$ > 3-5%”)

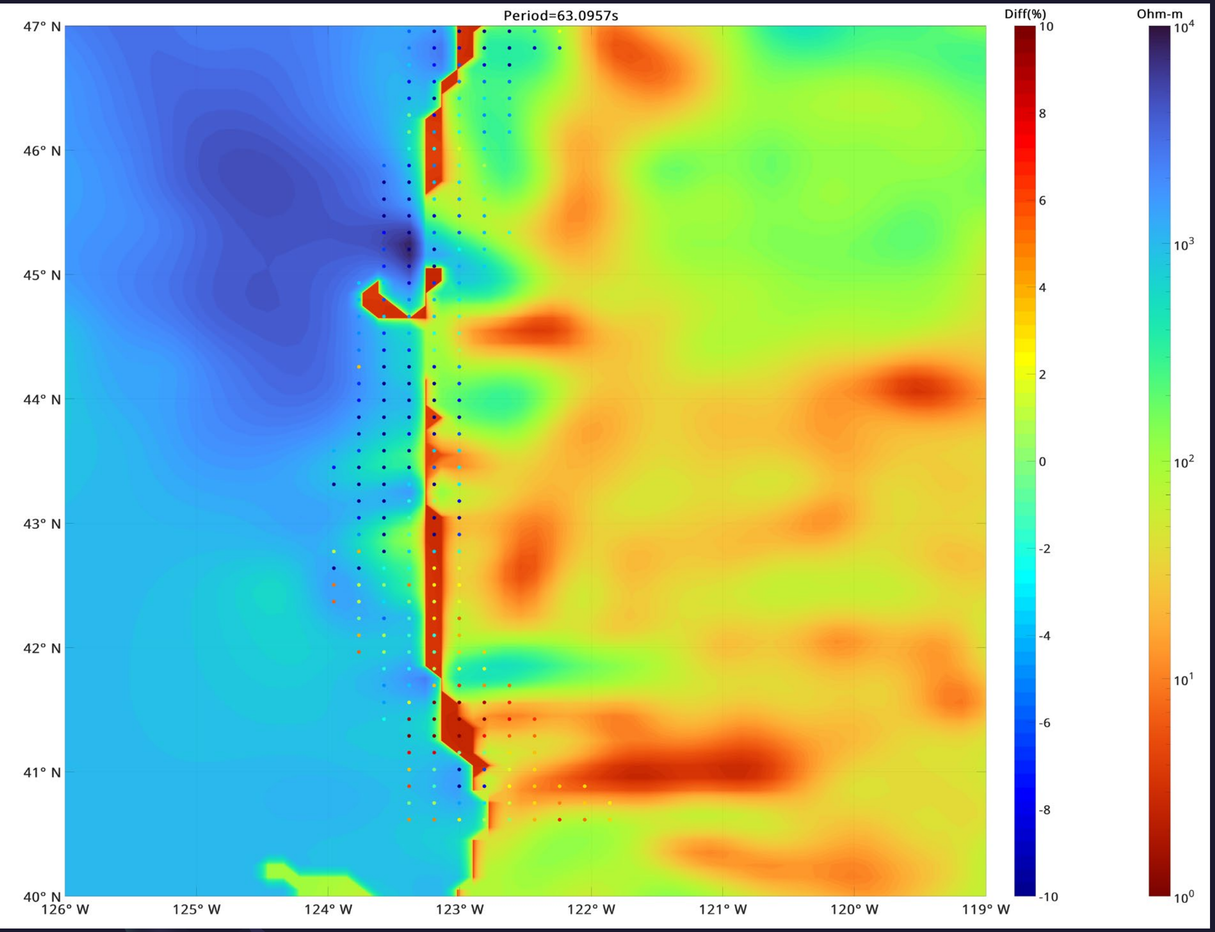


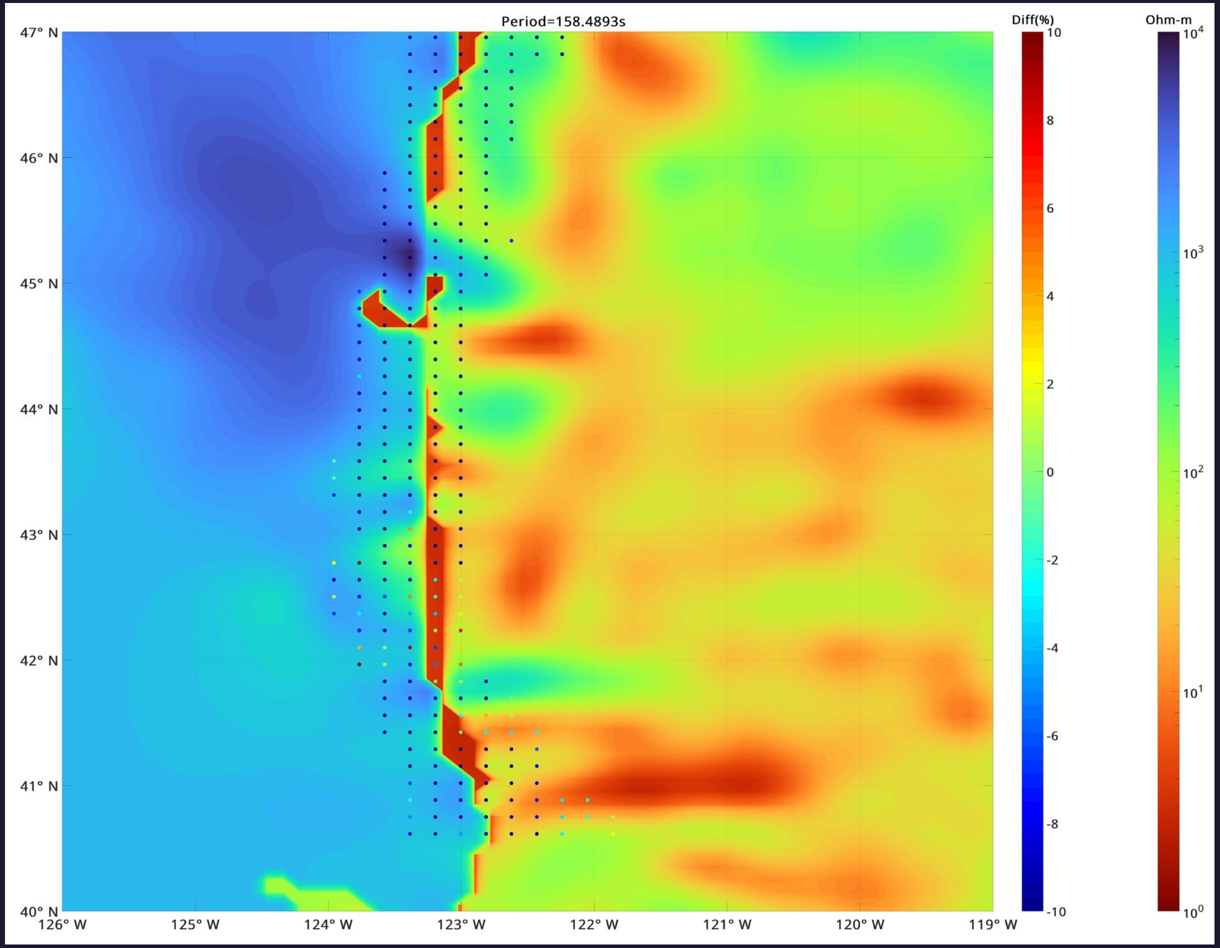

# Max. Phase Tensor Difference in Degrees: model 1,change in response at 63 s and 158 s period (“detectible if $\Delta\vartheta > 3\text{-}5^{o}$”)

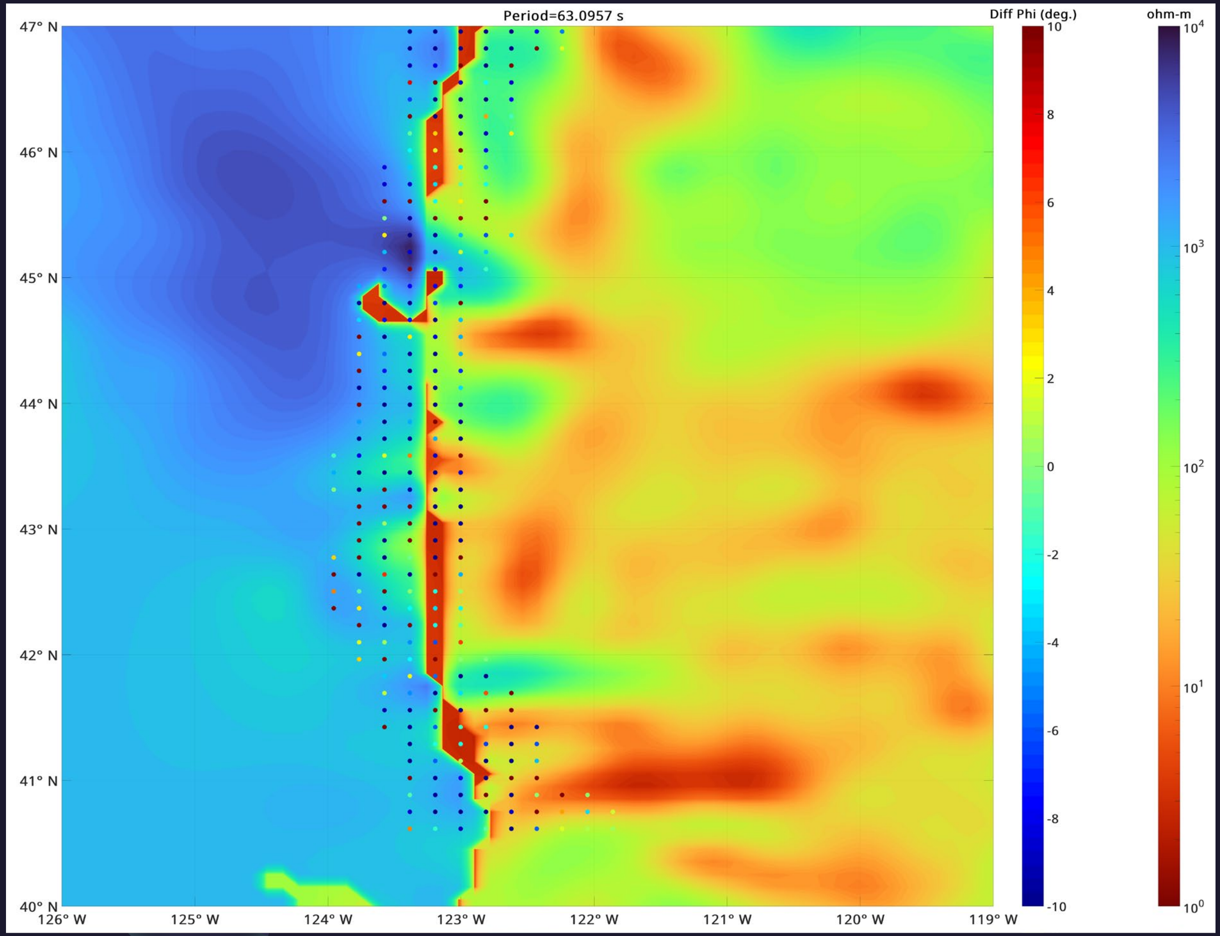


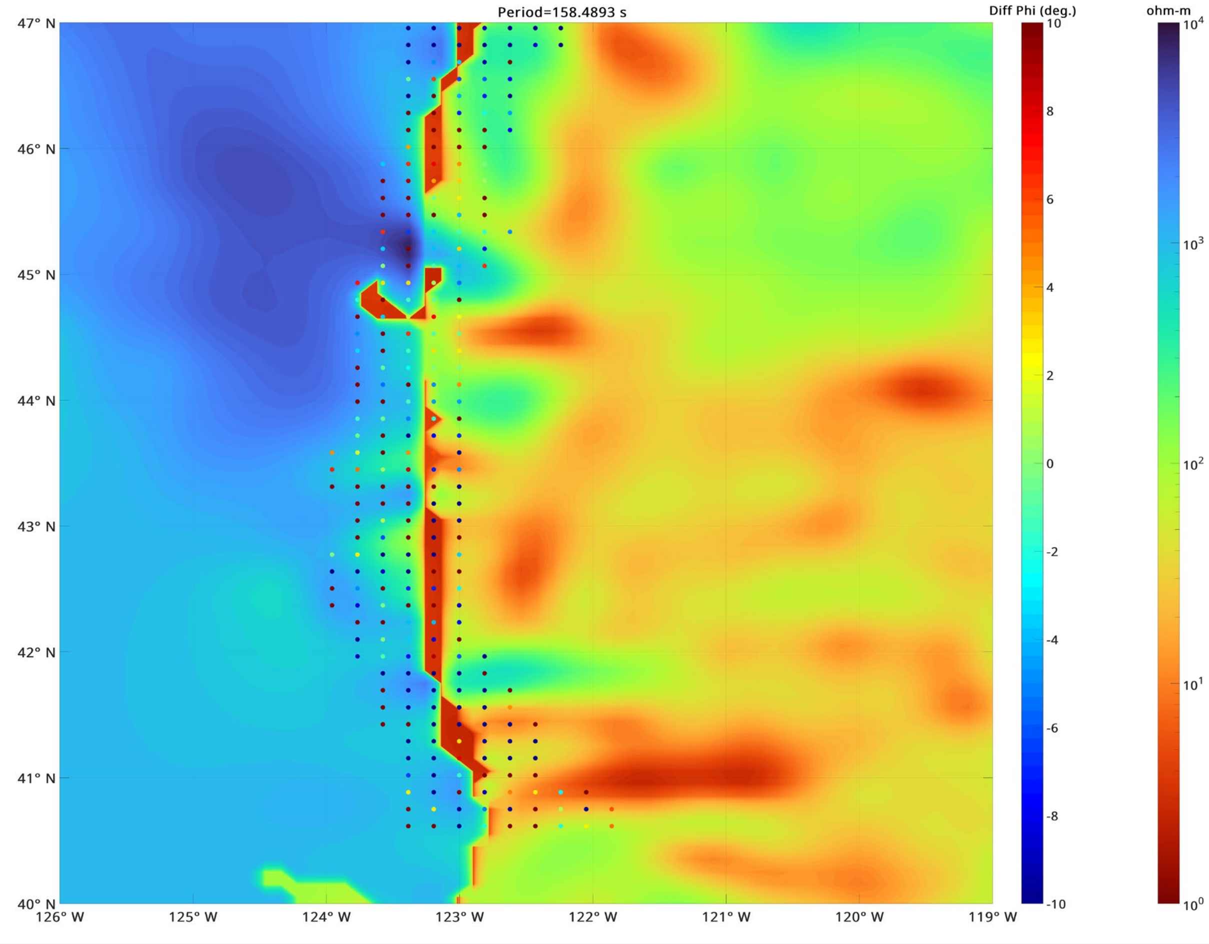

# Model 4 sensitivity to localized changes in cememtation factor

Resistivity right above slab interface

Cement factor: 1.7

Modify only a small segment along central Oregon margin

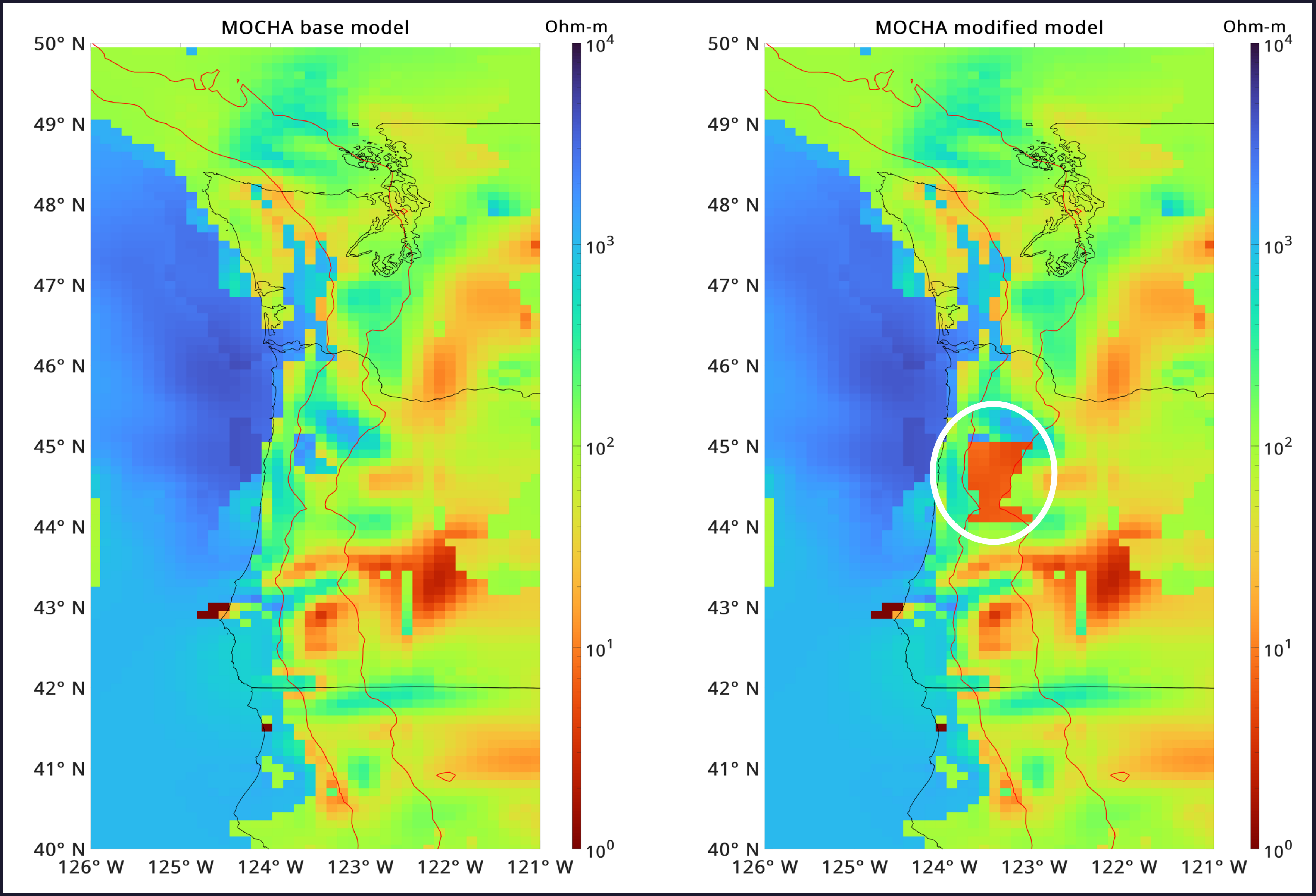

# MT Response: model 4

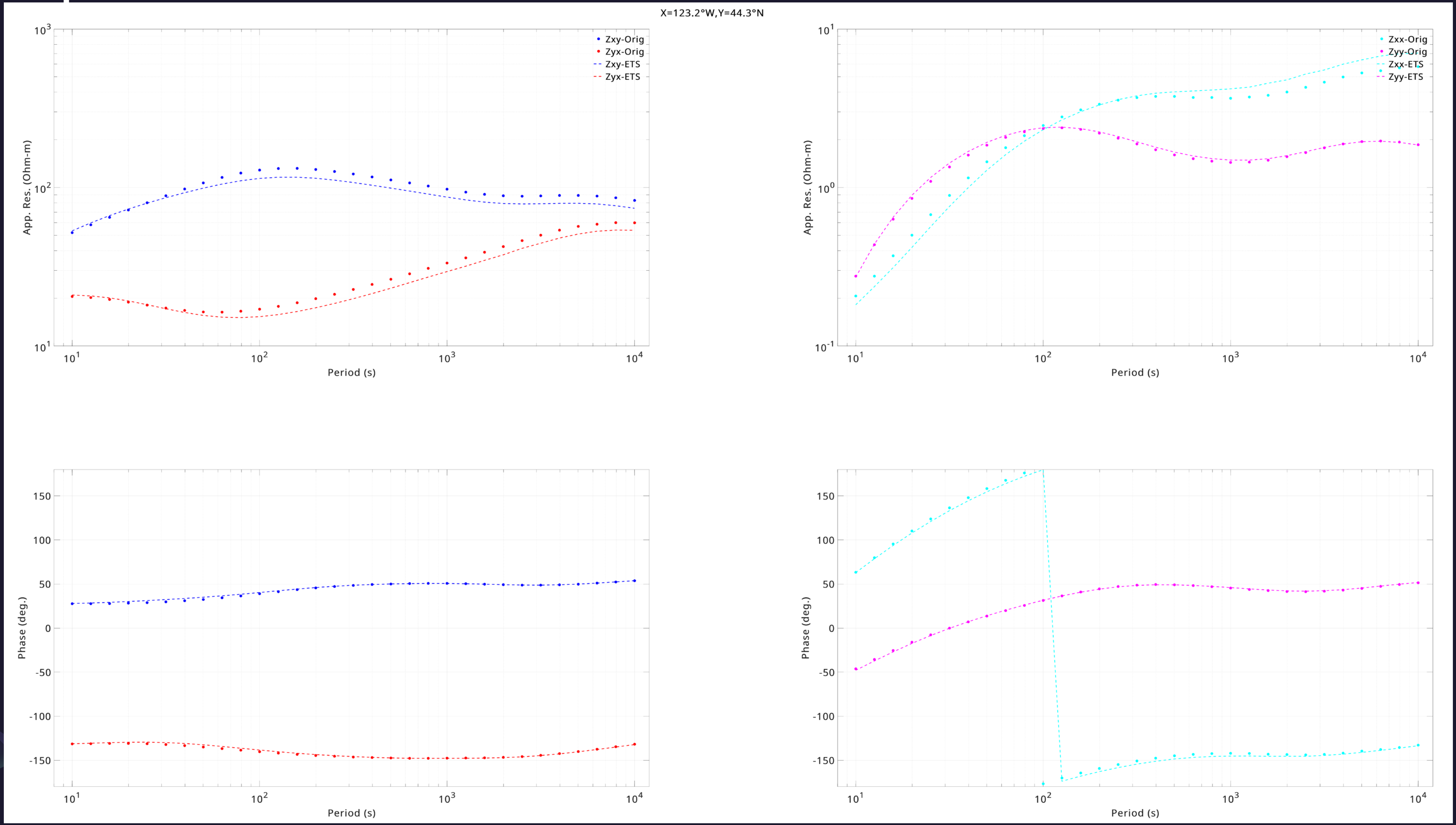

# App. Resistivity Difference: model 4

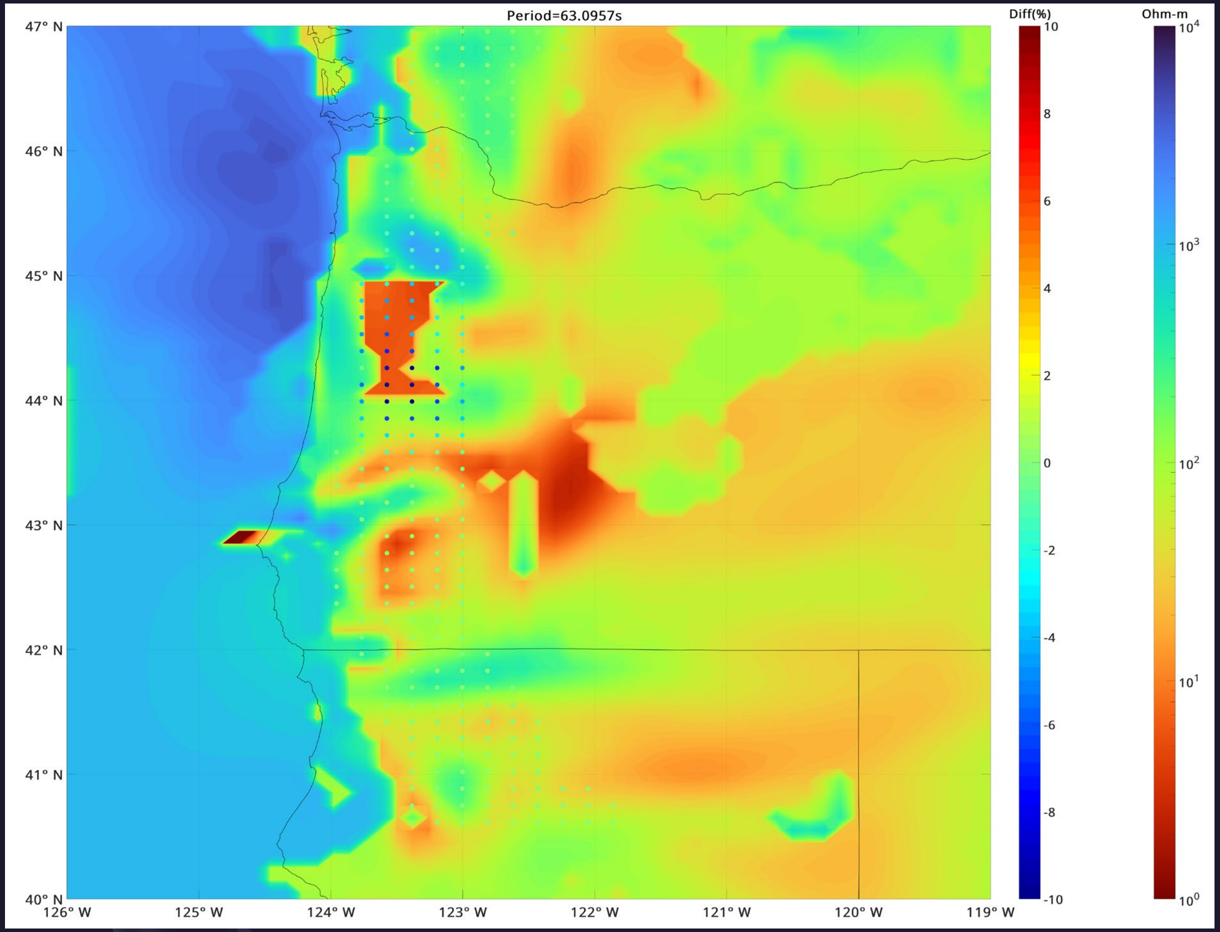


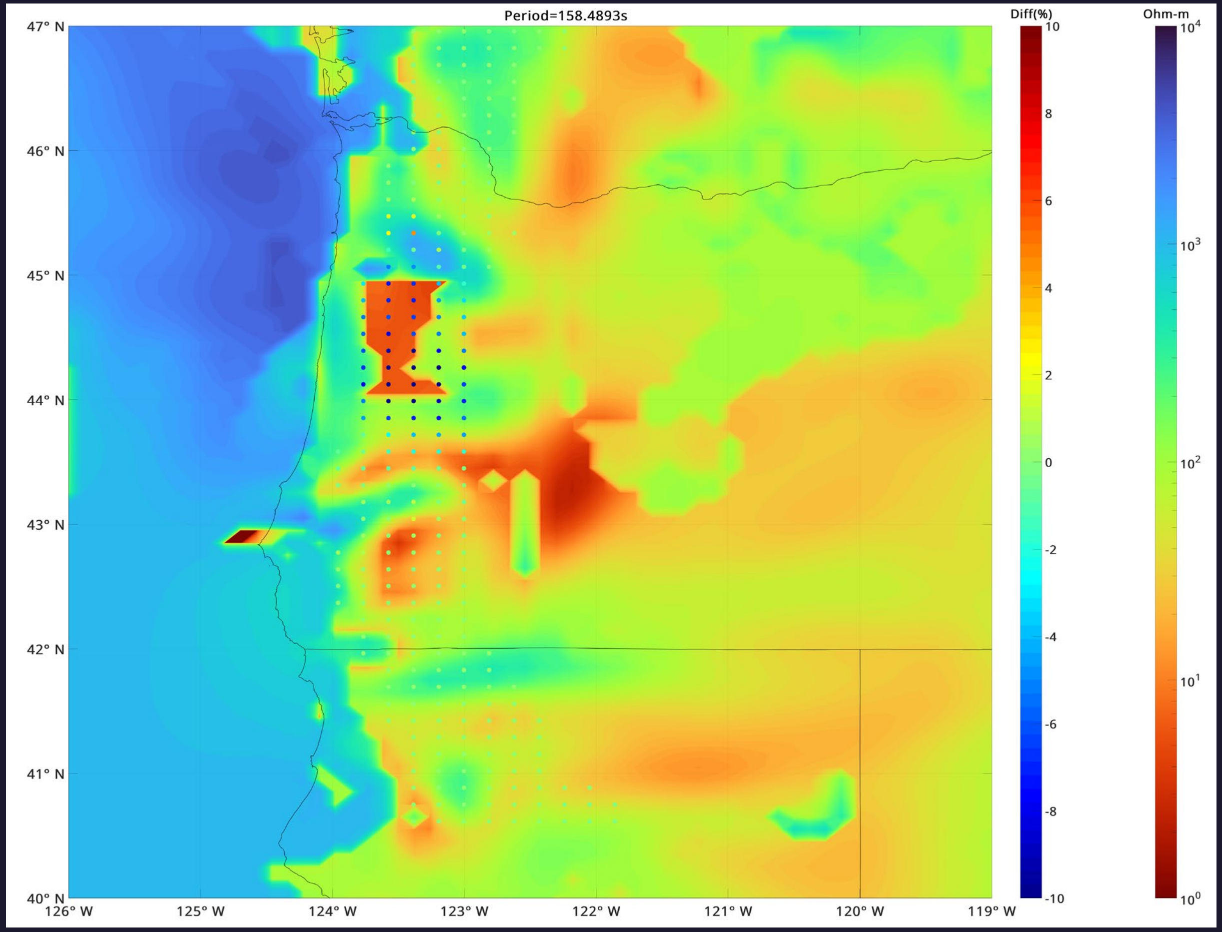

# App. Resistivity Difference: model 4

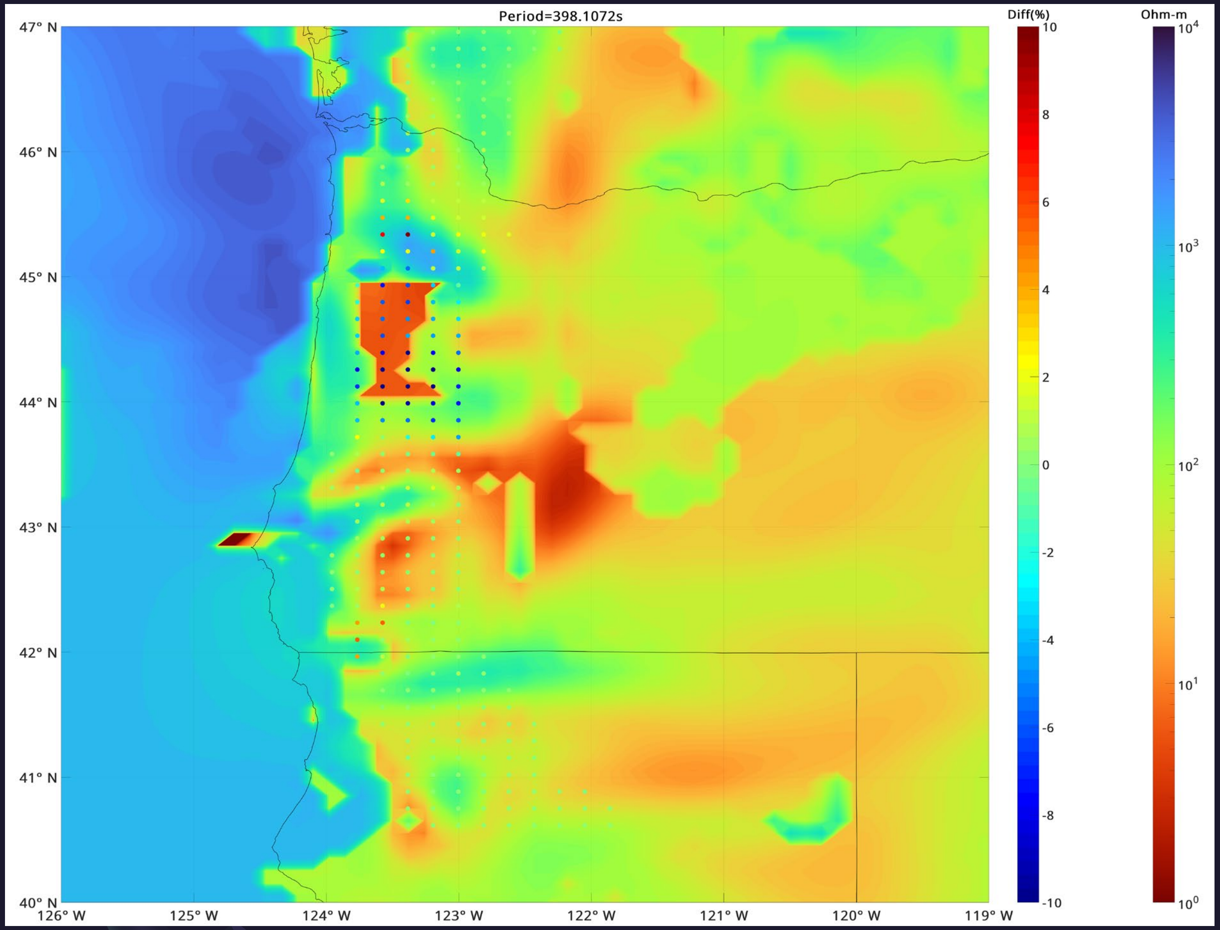


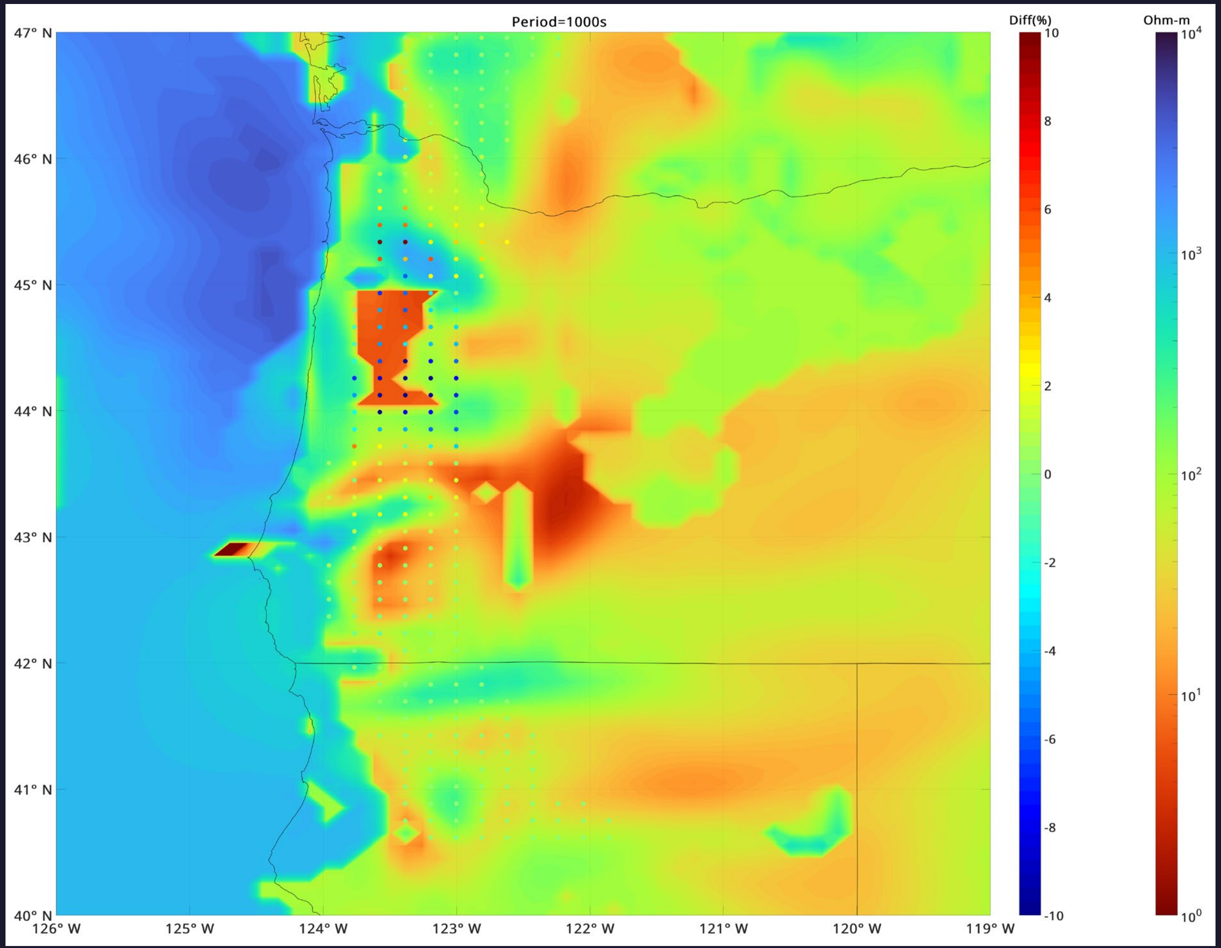

# Phase Tensor Difference: model 4

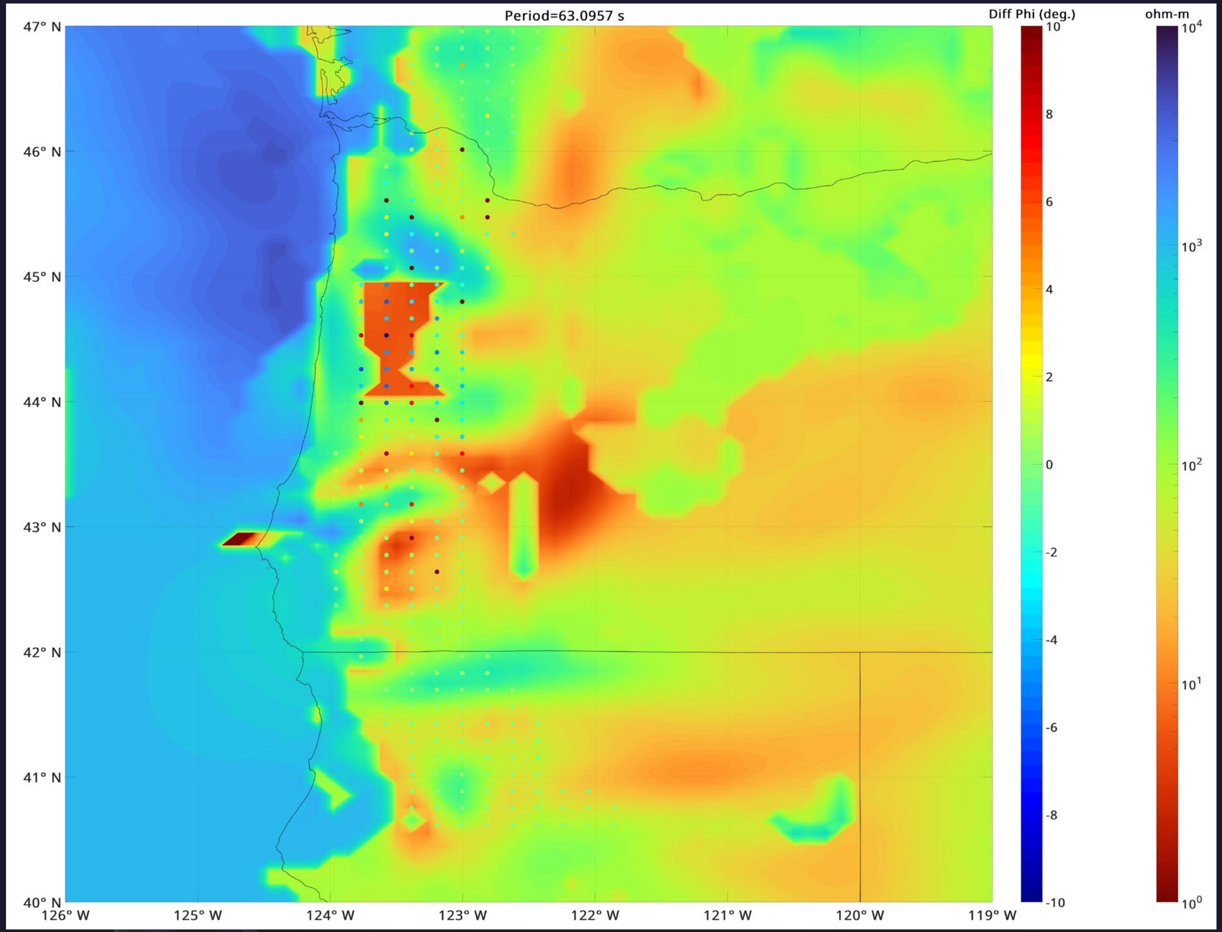


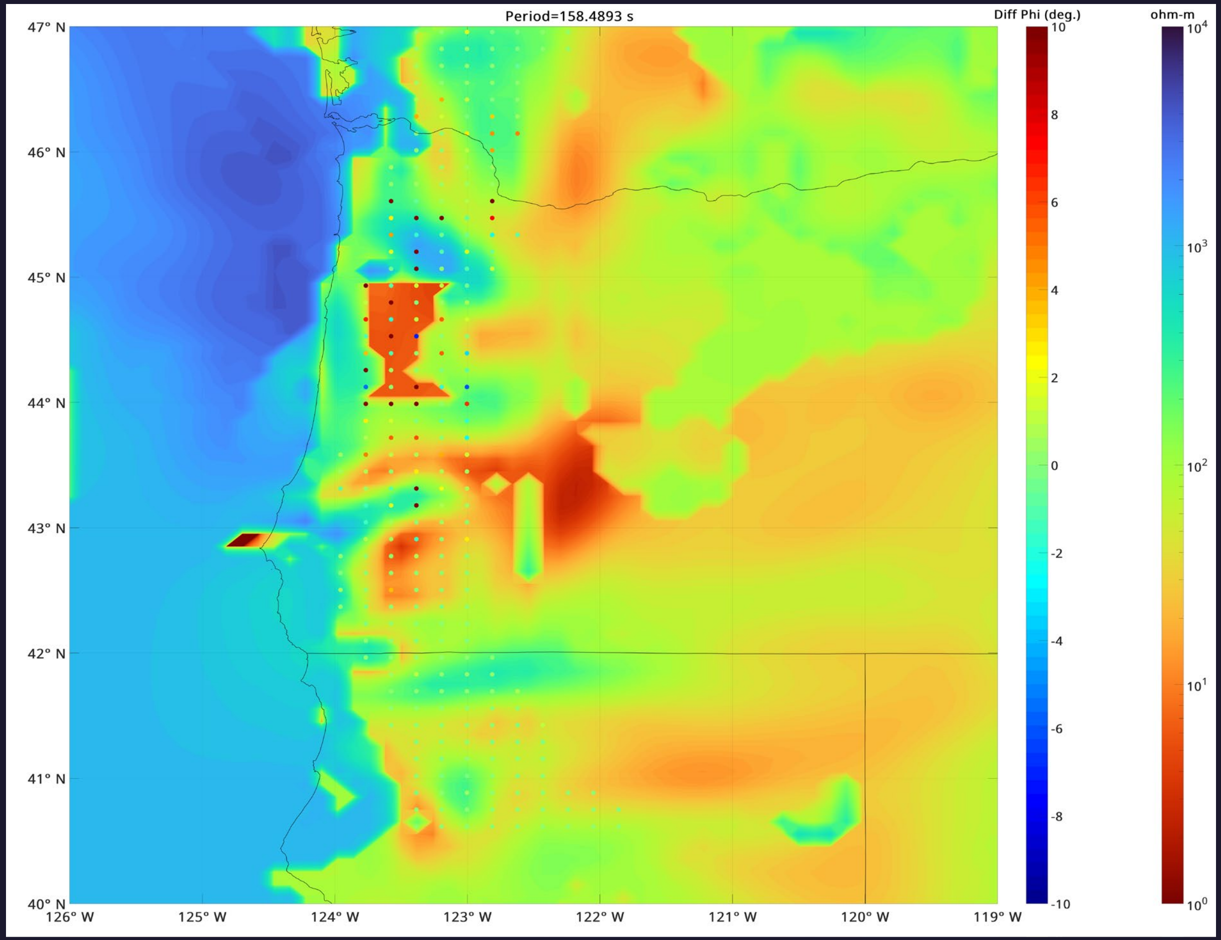

# Phase Tensor Difference: model 4

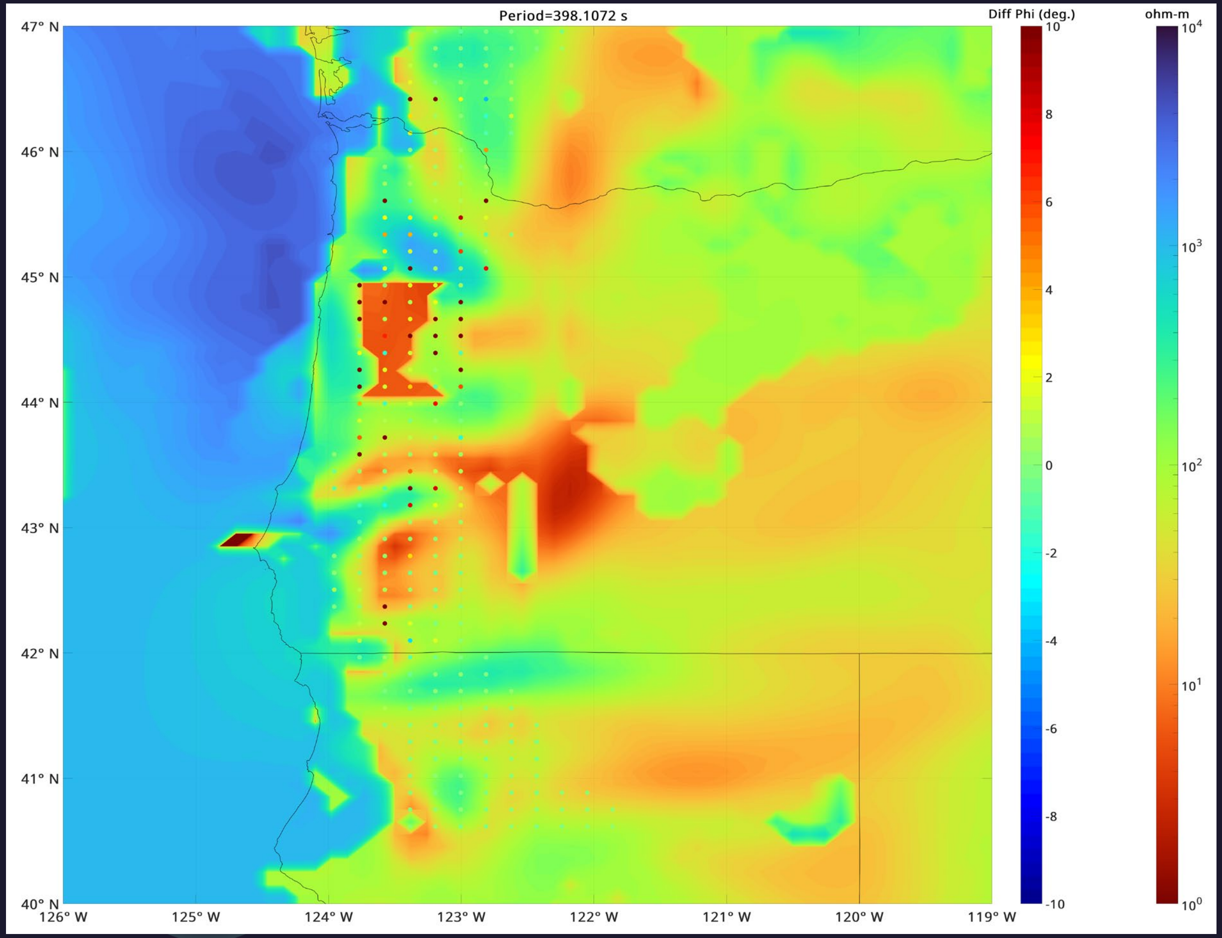


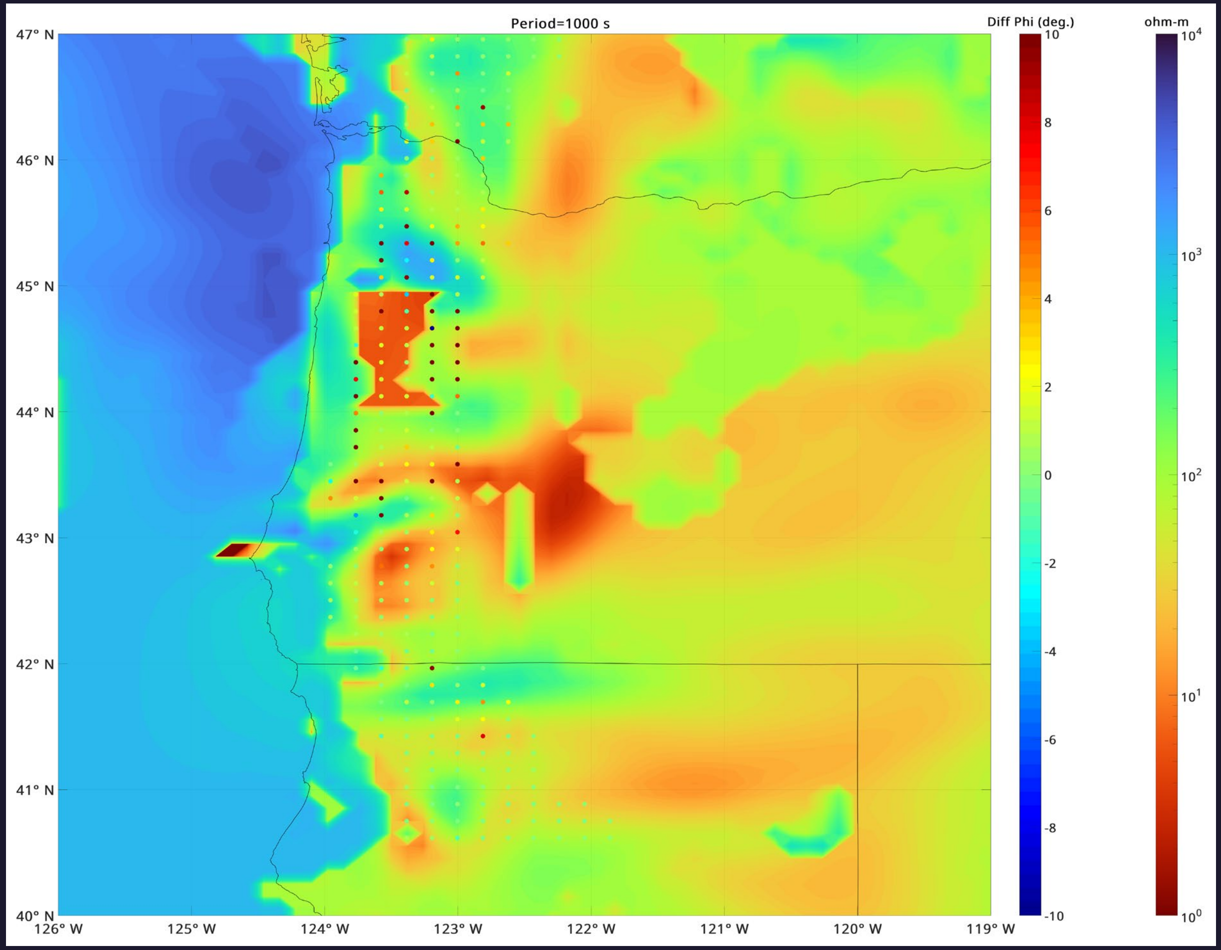

# Conclusions

Changes in the fluid/rock matrix in and near the boundary zone between the down-going slab and the mantle wedge, due either to

- mass fluid volume changes or to the
- realignment of the interconnected fluid network along mineral grain boundaries in response to changes in the stress field

during ETS cycles produce sufficiently large changes in the MT impedance tensor (i.e. apparent resistivity, phase, phase tensor) to be detectible from continuous MT monitoring,